Cell and Tissue Research (2020) 381:141–161
https://doi.org/10.1007/s00441-020-03182-0

REGULAR ARTICLE

Neural stem cell therapy of foetal onset hydrocephalus using the HTx rat as experimental model

Roberto Henzi[1,2] · Karin Vío[1] · Clara Jara[1] · Conrad E. Johanson[3] · James P. McAllister[4] · Esteban M. Rodríguez[1] · Montserrat Guerra[1]

Received: 22 October 2019 / Accepted: 28 January 2020 / Published online: 17 February 2020

Abstract

Foetal onset hydrocephalus is a disease starting early in embryonic life; in many cases it results from a cell junction pathology of neural stem (NSC) and neural progenitor (NPC) cells forming the ventricular zone (VZ) and sub-ventricular zone (SVZ) of the developing brain. This pathology results in disassembling of VZ and loss of NSC/NPC, a phenomenon known as VZ disruption. At the cerebral aqueduct, VZ disruption triggers hydrocephalus while in the telencephalon, it results in abnormal neurogenesis. This may explain why derivative surgery does not cure hydrocephalus. NSC grafting appears as a therapeutic opportunity. The present investigation was designed to find out whether this is a likely possibility. HTx rats develop hereditary hydrocephalus; 30–40% of newborns are hydrocephalic (hyHTx) while their littermates are not (nHTx). NSC/NPC from the VZ/SVZ of nHTx rats were cultured into neurospheres that were then grafted into a lateral ventricle of 1-, 2- or 7-day-old hyHTx. Once in the cerebrospinal fluid, neurospheres disassembled and the freed NSC homed at the areas of VZ disruption. A population of homed cells generated new multiciliated ependyma at the sites where the ependyma was missing due to the inherited pathology. Another population of NSC homed at the disrupted VZ differentiated into βIII-tubulin+ spherical cells likely corresponding to neuroblasts that progressed into the parenchyma. The final fate of these cells could not be established due to the protocol used to label the grafted cells. The functional outcomes of NSC grafting in hydrocephalus remain open. The present study establishes an experimental paradigm of NSC/NPC therapy of foetal onset hydrocephalus, at the etiologic level that needs to be further explored with more analytical methodologies.

Keywords Congenital hydrocephalus · Neurospheres · Neural stem cells · Transplantation · Ventricular zone disruption · Homing · Ependymogenesis · Repair

Introduction

Foetal onset hydrocephalus is a disease with multiple triggers. Gene mutations and environmental factors, such as vitamin B or folic acid deficiency (Jellinger 1986), intraventricular haemorrhage, prematurity-related germinal matrix haemorrhage (Boop 2004) and viral infection of ependyma (Johnson et al. 1967), can all trigger, separately, the onset of foetal hydrocephalus. A strong body of evidence substantiates the concept that foetal onset hydrocephalus is not only a disorder of CSF dynamics but also a brain disorder leading to a severe neurological impairment (Rodríguez et al. 2019). In 2001, Miyan and his co-workers asked a key question: "Humanity lost: the cost of cortical maldevelopment in hydrocephalus. Is there light ahead?"

Over the past 20 years, our investigations have been aimed to answer a relevant question: how can we explain the inborn

Roberto Henzi and Karin Vío both qualify as first authors.

Dedicated to Prof. Michael Pollay for his enthusiastic support to carry out the present research.

✉ Montserrat Guerra
monserratguerra@uach.cl

[1] Instituto de Anatomía, Histología y Patología, Facultad de Medicina, Universidad Austral de Chile, Valdivia, Chile

[2] Present address: Centro de Investigaciones Biomédicas, Facultad de Medicina, Universidad de los Andes, Santiago, Chile

[3] Department of Neurosurgery, Alpert Medical School at Brown University, Providence, RI, USA

[4] Department of Neurosurgery Division of Pediatric Neurosurgery, Washington University and the Saint Louis Children's Hospital, St. Louis, MO, USA

and, so far, irreparable neurological impairment of children born with hydrocephalus? (Rodríguez et al. 2012, 2019). We and others obtained evidence that the common history of hydrocephalus and brain maldevelopment starts early in the embryonic life with the disruption of the ventricular (VZ) and sub-ventricular (SVZ) zones (Guerra et al. 2015; Jiménez et al. 2001; Rodríguez et al. 2012, 2019). Such a disruption progresses as a wave from caudal to rostral regions of the developing ventricular system, following spatial and time courses; when striking the cerebral aqueduct, it results in aqueduct stenosis/obliteration and hydrocephalus, while when reaching the telencephalon, it leads to abnormal neurogenesis (Jiménez et al. 2001; McAllister et al. 2017; Rodríguez et al. 2012). Yet, the nature, mechanisms and extent of the brain impairment linked to hydrocephalus are far from been fully characterized. A treatment for hydrocephalus *and* the associated neurological impairment will likely arise from a better understanding of the biological basis of the brain abnormalities in hydrocephalus (Del Bigio 2001; McAllister et al. 2015; Williams et al. 2007). This view appears as one of the "lost highways" in hydrocephalus research, as described by Jones and Klinge (2008).

The disruption of the VZ may be triggered by the mutation of a series of genes, or by signals extrinsic to the VZ cells, such as intraventricular haemorrhage or changes in the CSF proteins. The common feature of these triggers is that they all affect the intracellular vesicle trafficking in the VZ cells (NSC and ependyma) resulting in abnormal cell junctions and loss of VZ integrity (Ferland et al. 2009; Klezovitch et al. 2004; Ma et al. 2007; Rasin et al. 2007; Rodríguez and Guerra 2017). In the VZ cells, N-cadherin and connexin 43 fail to reach the plasma membrane to form efficient adherent and gap junctions resulting in the disassembling of the VZ (Guerra et al. 2015; McAllister et al. 2017; Rodríguez et al. 2012, 2019). The VZ disruption occurs during the embryonic life and the perinatal period, affecting equally the neural stem cells (NSCs) and the multiciliated ependymal cells. The junction pathology similarly affects NSC and ependyma resulting in VZ disruption and ependymal denudation (Guerra et al. 2015; McAllister et al. 2017). The mutation of a series of genes involved in intracellular trafficking, environmental factors (folic acid deficiency) and intraventricular haemorrhage all finally result in a "stormy" intracellular traffic leading to a junction pathology, VZ disruption and two inseparable phenomena: hydrocephalus and abnormal neurogenesis. This body of evidence leads us to conclude that foetal onset hydrocephalus is, essentially, a cell junction pathology of NSC (Rodríguez et al. 2012, 2019).

Derivative surgery is intended to minimize brain damage resulting from hydrocephalus but it cannot solve the inborn neurological impairment caused by the brain maldevelopment associated with NSC pathology. Keeping in mind that foetal onset hydrocephalus is, essentially, a NSC pathology and that in cases of hereditary hydrocephalus, such a pathology is an intrinsic defect of these cells (Guerra et al. 2015), the transplantation of normal NSC into the CSF of foetuses or neonates developing hydrocephalus to repair VZ disruption and sequelae appears as a goal worth pursuing.

Stem cell transplantation represents an opportunity for treating many neurological diseases (Bjorklund and Kordower 2013; Lindvall and Kokaia 2006, 2010; Lindvall et al. 2004). In early investigations, the stem cells were grafted into the brain parenchyma, close to the injured or altered region. Stem cell delivery into the CSF is emerging as an alternative, particularly for diseases with a broad distribution in the CNS (Bai et al. 2003; Neuhuber et al. 2008; Pluchino et al. 2003; Wu et al. 2002).

Beside our preliminary reports (Rodríguez and Guerra 2017; Rodríguez et al. 2019), we know of no other investigations using NSC grafting in hydrocephalic animal models. HTx rats develop hereditary congenital hydrocephalus (hyHTx). In this animal model, VZ disruption occurs between E19 and PN10 as multiple and growing foci of disruption, resembling the situation in human hydrocephalic foetuses (Guerra et al. 2015; Ortloff et al. 2013). This allows NSC grafting to be performed postnatally, while the VZ disruption is still in progress. A question we raised before performing NSC grafting into the ventricle of HTx rats was whether the hydrocephalic CSF, with its abnormal protein composition (Ortloff et al. 2013), would be a friendly medium to host the grafted NSC. This seems to be the case, since neurospheres (NEs) obtained from non-affected HTx (nHTx) rats when cultured in the presence of CSF from hyHTx or nHTx rats differentiate into neurons, astrocytes and ependyma (Henzi et al. 2018).

The first aim of the present investigation is to find the appropriate grafting conditions regarding the type and number of NE, the surgery procedure and the age of hyHTx rats

Fig. 1 NSC/NPC collected from the VZ/SVZ of nHTx grow into neurospheres (NEs) that can be grafted into a lateral ventricle of hyHTx rats. **a** Frontal section of a lateral ventricle (LV) of a PN1, nHTx rat immunostained for nestin. The ventricular and sub-ventricular zones of the dorsal and lateral (lw) walls of the ventricle are formed by nestin+, NSCs/NPCs, while the medial wall (mw) is lined by ependyma. **b** Protocol of the neurosphere assay. **c** Head of a PN1, hyHTx rat showing the translucent dilated lateral ventricles where the NEs are grafted (arrow). **d** Living 6DIV NEs visualized with phase contrast microscopy. **e** Nestin in block immunostaining of a 6DIV NE. **f** Paraffin section of 6DIV NEs immunostained for nestin. **g** 6DIV NE exposed to BrdU the last 12 h in culture. Immunofluorescence for BrdU. **h** 4DIV NEs exposed to BrdU the last 24 h in culture. **i** Paraffin section of the brain of a PN1, hyHTx rat grafted with 4 or 6 DIV NEs labelled with BrdU and killed 2 days later. Double immunofluorescence for nestin (red) and BrdU (green). BrdU-labelled NSCs/NPCs populate the region of VZ disruption. se, septum; st, striatum. Photo-montage. A picture of a 6DIV NE immunostained in block for caveolin has been pasted on figure i. *Inset*: disruption zone visualized with the channel for BrdU. Scale bar, **a** 250 μm; **c** 100 μm; **d** 40 μm; **e** 40 μm; **g** 40 μm; **h** 40 μm; **i** 200 μm, inset 55 μm; bar in pasted neurosphere 40 μm

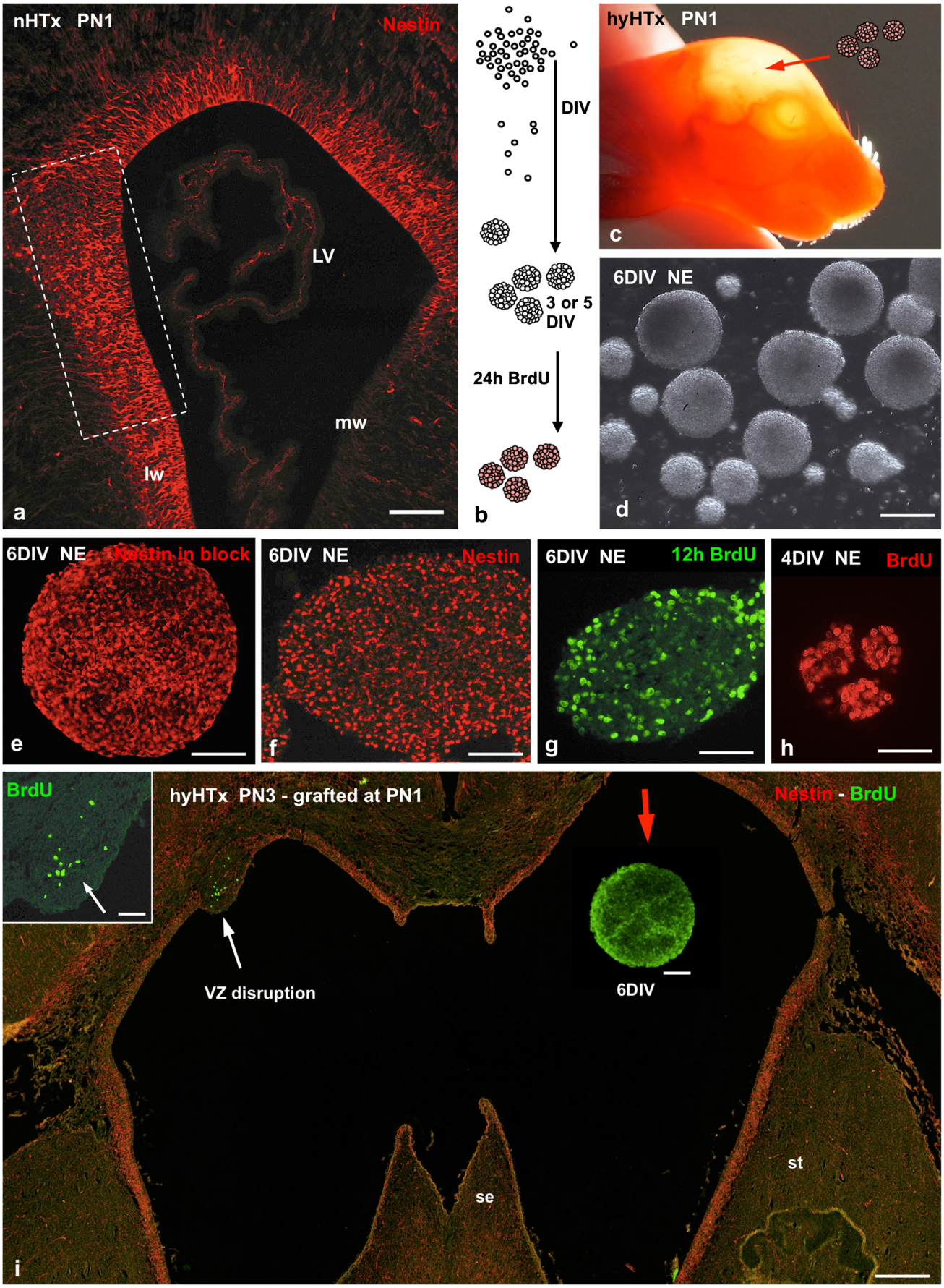
nHTx PN1
Nestin
LV
mw
lw
a
DIV
3 or 5 DIV
24h BrdU
b
hyHTx PN1
c
6DIV NE
d
6DIV NE
Nestin in block
e
6DIV NE
Nestin
f
6DIV NE
12h BrdU
g
4DIV NE
BrdU
h
BrdU
hyHTx PN3 - grafted at PN1
Nestin - BrdU
VZ disruption
6DIV
se
st
i

hosting the graft. The second aim is to establish the fate of the grafted NE and whether they would disassemble leaving NSC/NPC free in the CSF, as occurs in vitro. The final goal is to establish whether or not the grafted NSC/NPC would somehow make their way and home to the areas of VZ disruption and, hopefully, repair the disrupted VZ.

Materials and methods

Animals

Rats of the HTx strain donated by Prof. Hazel Jones (University of Florida, Gainesville) in 2002 were bred into a colony in the Animal Facility at the Instituto de Anatomía Histología y Patología, Universidad Austral de Chile, Valdivia. The colony is maintained by mating phenotypically normal siblings; in each offspring, 30–40% of newborns carry the hydrocephalic phenotype. Housing, handling, care and processing of animals were carried out according to regulations of the National Research Council of Chile (Conicyt). The ethics committee of Universidad Austral de Chile approved the experimental protocol. The hydrocephalic phenotype was identified from an overtly domed head and by transillumination of the head of newborns and later confirmed by microscopic examination of brain. The pathology expressed by the subcommissural organ was used as a phenotypic landmark (Ortloff et al. 2013).

Neurosphere assay

Neural stem (NSC) and neural progenitor (NPC) cells obtained from PN1 nHTx rats were cultured to obtain neurospheres, as described by Guerra et al. (2015) (Fig. 1a–e). The dorsal and lateral walls of the lateral ventricles containing the ventricular (VZ) and sub-ventricular (SVZ) zones were dissected and soaked in Neurocult NS-A proliferation Medium-Rat, supplemented with 20 ng/ml EGF and 2 μg/ml heparin (Stem Cell Technologies, Vancouver, CA) and antibiotics (penicillin 100 μg/ml and streptomycin 100 μg/ml (Sigma). Later, the tissue was transferred to an Eppendorf tube and disaggregated mechanically using a P-200 micropipette. The cell suspension was centrifuged for 10 min at 110 *g*; the resulting pellet was diluted (1:10) with culture medium. The viable cells were counted using the trypan blue cell viability assay; 60,000 cells/ml were seeded in a non-adherent 12-well culture plate (TPP; Techno Plastic Products AG, Trasadingen, Switzerland). The cells were cultured for 4 or 6 days (DIV, days in vitro); 10 μM BrdU was added for the last 24 h of culture, as described by Henzi et al. (2018). The cells were studied daily by phase contrast microscopy (Nikon Diaphot Inverted Tissue Culture Microscope). At 4DIV and 6DIV, photographs were obtained.

4DIV and 6DIV neurospheres, exposed to BrdU for the last 24 h in culture, were fixed in Bouin fluid, embedded in paraffin and serially cut. Sections were processed for immunofluorescence using anti-BrdU and anti-nestin.

Neurosphere grafting

Approximately 100 neurospheres of 4DIV were grafted into a lateral ventricle of PN1 ($n = 10$) and PN2 ($n = 2$) hyHTx rats and 30 neurospheres of 6DIV were grafted in PN7 hyHTx ($n = 50$) rats. In the group of PN7 hyHTx rats hosting the graft, the donor rats were nHTx littermates; in the groups PN1 and PN2 of grafted hyHTx rats, the donor nHTx rats were from different litters. Approximately 400 NSC formed each 4DIV neurosphere; thus, each PN1 host was grafted with about 40,000 NSCs. Each 6DIV contains about 4000 cells, 70% of which were NSCs and 30% were committed cells (Henzi et al. 2018); thus, each PN7 host was grafted with about 120,000 cells (80,000 NSCs). The brains of the operated rats were microscopically scanned through series of sections (see below).

Surgery hyHTx rats were anesthetized using a combination of ketamine (40 mg/kg) and acepromazine (100 mg/kg). The skull was cleaned with 70° ethanol and iodine. A 10-μl Hamilton syringe containing the neurospheres was connected through a cannula to a 30-G needle. The needle was inserted into the right lateral ventricle of the brain, 0.5 mm posterior to bregma and 1.5 mm lateral to the sagittal suture. After the needle had penetrated 1.5 mm from the meninges, it was

Fig. 2 Fifteen minutes after grafting into the ventricle of PN7 hyHTx rats, NEs remain proliferative and free inside the dilated ventricles. **a** Immunostaining for BrdU and background staining with haematoxylin (BrdU-H). 6DIV NEs grafted into the dilated ventricles of a PN7 hyHTx rat accumulate in the ventral horns of the lateral ventricle. Area framed is shown in (a'). se, septum; st, striatum. The cannula with NE inside is a photo-montage. **a'** NE lying free in the ventral horn of ventricle. The lateral wall of ventricle is lined by VZ cells (VZ) and the medial wall by ependyma (E). Area framed is shown in (a"). **a"** Most cells of NE are labelled with BrdU. The arrow points to unlabelled cells. **b** Detailed magnification of two NE 15 min after grafting. LV, lateral ventricle. Area framed is shown in (b'). **b'** Arrow points to a mitosis with the chromosomes labelled with BrdU. **c** Grafted NE showing a mitotic figure (arrow). **d, d'** 6DIV NE 15 min after grafting. Most cells are BrdU+ and nestin+. Asterisk in (d) points to a NE shown in (d'). VZ, ventricular zone; E, ependyma. **e, e'** Grafted NEs contain few βIII-tubulin+ cells. **f, f'** A few cells of grafted NE contain βIV-tubulin+ particles. **f"** Same picture as in (f') visualized with the channel for βIV-tubulin. Arrows in (f') and (f") point to a cell reactive for βIV-tubulin. **g**, **h** Two days after grafting 4DIV (**g**) and 6DIV (**h**) NEs, clusters of BrdU+ cells appeared along the lateral wall of ventricle (g) and close to the areas of VZ disruption in the dorsal wall and lining the denuded area (h). **i** A large cluster of BrdU+ cells has penetrated through a disrupted area of VZ and labelled cells are invading the neighbour tissue. Scale bar, **a** 500 μm; **a'** 26 μm; **a"** 10 μm; **b** 35 μm; **b'** 10 μm; **c** 7 μm; **d**, **e**, **f** 80 μm; **d'**, **e'** 12 μm; **f'** 10 μm; **f"** 10 μm; **g** 40 μm; **h** 50 μm; **i** 70 μm

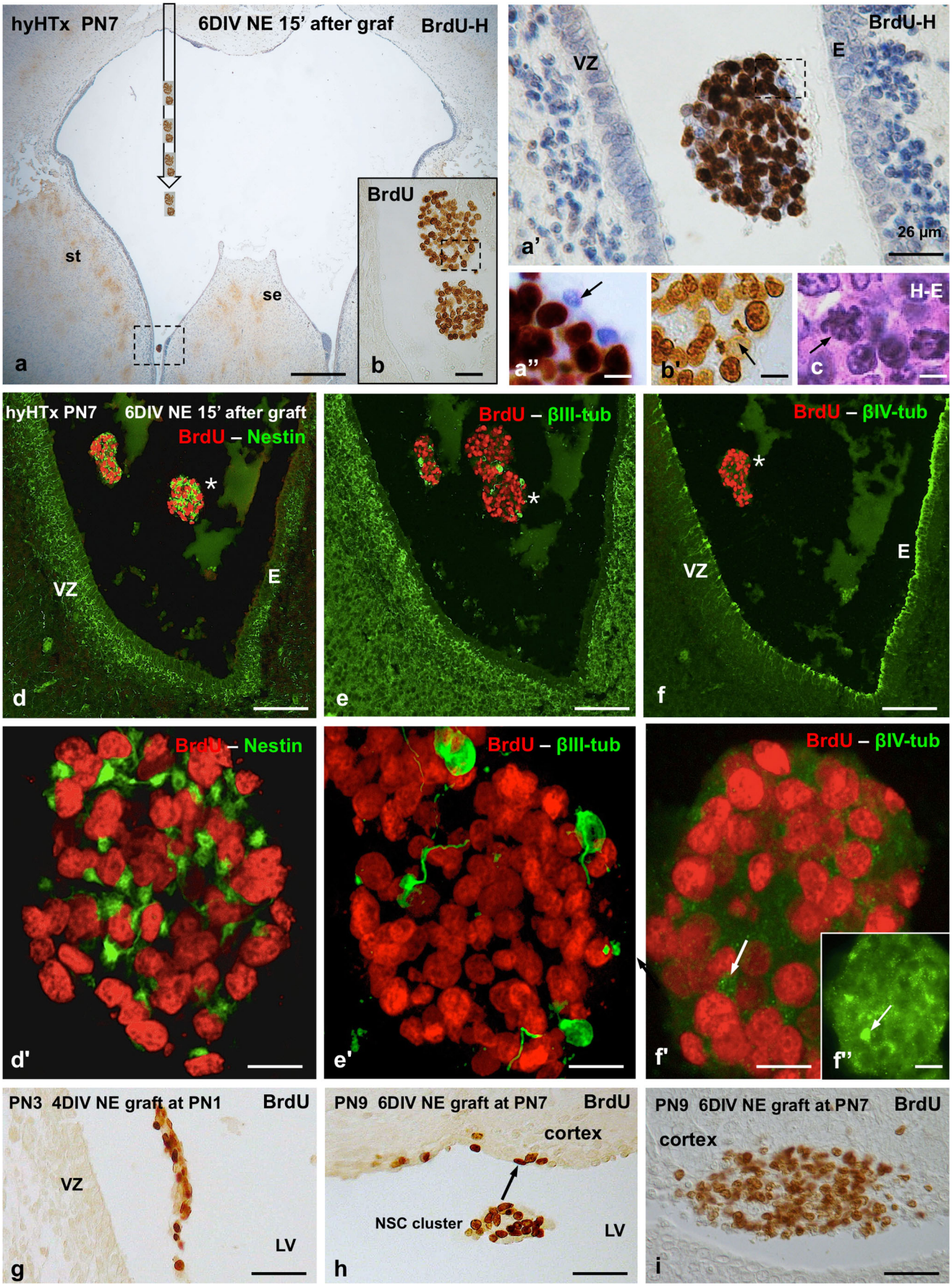
hyHTx PN7
6DIV NE 15' after graf
BrdU-H
st
se
BrdU
a
b
VZ
E
BrdU-H
26 µm
a'
a''
b'
H-E
c
hyHTx PN7
6DIV NE 15' after graft
BrdU – Nestin
VZ
E
d
BrdU – βIII-tub
e
BrdU – βIV-tub
VZ
E
f
BrdU – Nestin
d'
BrdU – βIII-tub
e'
BrdU – βIV-tub
f'
f''
PN3 4DIV NE graft at PN1
BrdU
VZ
LV
g
PN9 6DIV NE graft at PN7
BrdU
cortex
NSC cluster
LV
h
PN9 6DIV NE graft at PN7
BrdU
cortex
i

oriented towards the posterior horns at an angle of approximately 45–50°. The 10 μl of culture medium containing the neurospheres was sub-perfused during 5 min. After the injection, the needle was held in place for 2 min to prevent the grafted NE from flowing back and out of the ventricle. Animals were allowed to recover before returning them to the litter.

Sampling

The grafted animals were euthanized at different time intervals: 15 min ($n = 22$), 2 days ($n = 27$), 7 days ($n = 11$) and 19 days ($n = 2$) after surgery. The rats were anesthetized as for surgery (see above) and the head was fixed by vascular perfusion with Bouin's fluid (Baker 1977) for 20 min; then the brain was dissected out and further fixed by immersion in Bouin's fluid, for 2 days. Embedding was in paraffin. Serial coronal sections, 7 μm thick, were obtained through the whole brain. Each series contained about 300–500 sections; every tenth section of the series was mounted side-by-side on the same slides, thus giving ten semi-series of sections that were used for haematoxylin-eosin staining and for immunocytochemistry. Each semi-series represented a scanning throughout the whole brain. This procedure also allowed studying adjacent sections with different antibodies. Twenty-nine experiments were regarded successful considering the presence of neurospheres or NSCs/NPCs in the ventricles: 15 min ($n = 13$), 2 days ($n = 10$), 7 days ($n = 4$) and 19 days ($n = 2$) after surgery.

The brains of PN1 nHTx rats ($n = 6$) and of non-grafted hyHTx rats, E20 ($n = 5$), PN1 ($n = 10$) and PN7 ($n = 4$), were fixed in Bouin's and embedded in paraffin. The sections were stained with haematoxylin-eosin or immunostained for nestin.

Immunohistochemistry

Sections were processed for immunohistochemistry by the peroxidase-anti-peroxidase (PAP) method, described by Sternberger et al. (1970), or the streptavidin/biotin method (Vectastain kit; Vector, Serva, Heidelberg, Germany), with diaminobenzidine (Sigma, St. Louis, MO, USA) as electron donor. Anti-bromodeoxyuridine (BrdU) monoclonal antibody (Developmental Studies Hybridoma Bank, Iowa, IA, USA) was used as the primary antibody and anti-mouse IgG developed in rabbits, as the secondary antibody. The antibodies were diluted in 0.1 M Tris buffer, pH 7.8, containing 0.7% non-gelling seaweed gelatin lambda carrageenan and 0.5% Triton X-100 (both from Sigma). Incubation was for 18 h at room temperature. Endogenous peroxidase activity was blocked by pre-incubating the sections in 3% hydrogen peroxide in cold methanol, for 10 min. BrdU immnunoreactivity was enhanced by incubating the sections in 20 mM citrate buffer, pH 6.0, followed by three cycles of microwave irradiation at 90 °C, 4 min each. After cooling to room temperature, sections were washed 3 times in Tris-HCl buffer, pH 7.8. Omission of the primary antibody during incubation provided the control for the immunoreactions. Some sections were background-stained with haematoxylin.

Double immunofluorescence and confocal microscopy

Each semi-series of sections through the brain, containing adjacent sections, was processed for double immunofluorescence using pairs of antibodies. Antibodies against the following compounds were utilized: (i) BrdU (to track grafted cells), monoclonal (Developmental Studies Hybridoma Bank, USA), supernatant 1:500 dilution; (ii) BrdU (to track grafted cells), raised in rabbits (Rockland antibodies and assay, Limerick, PA, USA), 1:500 dilution; (iii) glial fibrillary acidic protein (GFAP, astrocyte marker), polyclonal raised in rabbit (Sigma), 1:750 dilution; (iv) βIII-tubulin (neuroblasts, NPC marker), monoclonal (Sigma), 1:750 dilution; (v) βIV-tubulin (multiciliated ependyma marker), monoclonal (Abcam, Cambridge, UK), 1:100 dilution; (vi) nestin (NSC marker), monoclonal (Developmental Studies Hybridoma Bank, Iowa, USA), supernatant, 1:20 dilution and (vii) N-cadherin (adherent junctions), raised in rabbit (Santa Cruz

Fig. 3 Two days after surgery, NSC of 4DIV neurospheres grafted into PN1, hyHTx rats selectively populate the areas of ventricular zone disruption. **a** Frontal section of the brain of a PN1, hyHTx rat showing the areas of VZ disruption (arrows). *Inset*: area of VZ disruption delimited by arrows. Haematoxylin-Eosin stain. **b** PN1, hyHTx 15 min after grafting 4DIV NE labelled with BrdU. Immunoperoxidase staining for BrdU. Range framed is shown in (c). **c** Detailed magnification of range framed in (b); 15 min after grafting NEs accumulate in the ventral horn of the dilated lateral ventricle. **d** PN3, hyHTx grafted with 4DIV NE at PN1. Haematoxylin-eosin stain. Area framed is shown in (c). se, septum; st, striatum. **e** Detailed magnification of area framed in (d), showing area of ventricular zone (VZ) disruption (between arrows). **f** Section adjacent to that of (d) processed for immunofluorescence for BrdU. Area framed is shown in (g, h). The grafted NSCs/NPCs (green) populate the disrupted VZ. **g** Double immunofluorescence for nestin (red) and BrdU (green) of area shown in (f). Laser microscopy. The arrow points to the disruption front of the ventricular zone (VZ). The grafted cells populate the disrupted area. *Left inset*: detailed view of a grafted cell expressing βIII-tubulin. *Right inset*: detailed magnification of a nestin+ cell framed in (g). **h** Double immunofluorescence for nestin (red) and BrdU (green) of area shown in (f). Fluorescence microscope combined with Nomarski optics. The arrow points to the disruption front. Asterisk indicates area shown in inset. *Inset*: detailed view of two nestin+ grafted cells. **I** Double immunofluorescence for βIV-tubulin (red) and BrdU (green) of area shown in (f). Arrow, disruption front. area framed is shown in inset. *Inset*: cluster of grafted cells attached to the free surface of VZ. **j**, **k** Cluster of grafted cells attached to the VZ express βIII-tubulin (**j**) and nestin (**k**). **l** The variation of the fluorescence intensity of the nuclei of grafted cells (1, 2) suggests dilution of label due to mitotic divisions. *Inset*: labelled nucleus probably undergoing mitosis. Scale bar, **a** 1 mm; **b** 1 mm; **c** 40 μm; **d** 1 mm, **e** 100 μm; **f** 450 μm; **g** 20 μm, left inset 5 μm, right inset 6 μm; **h** 25 μm, inset 7 μm; **i** 80 μm, inset 15 μm; **j** 20 μm; **k** 10 μm; **l** 17 μm

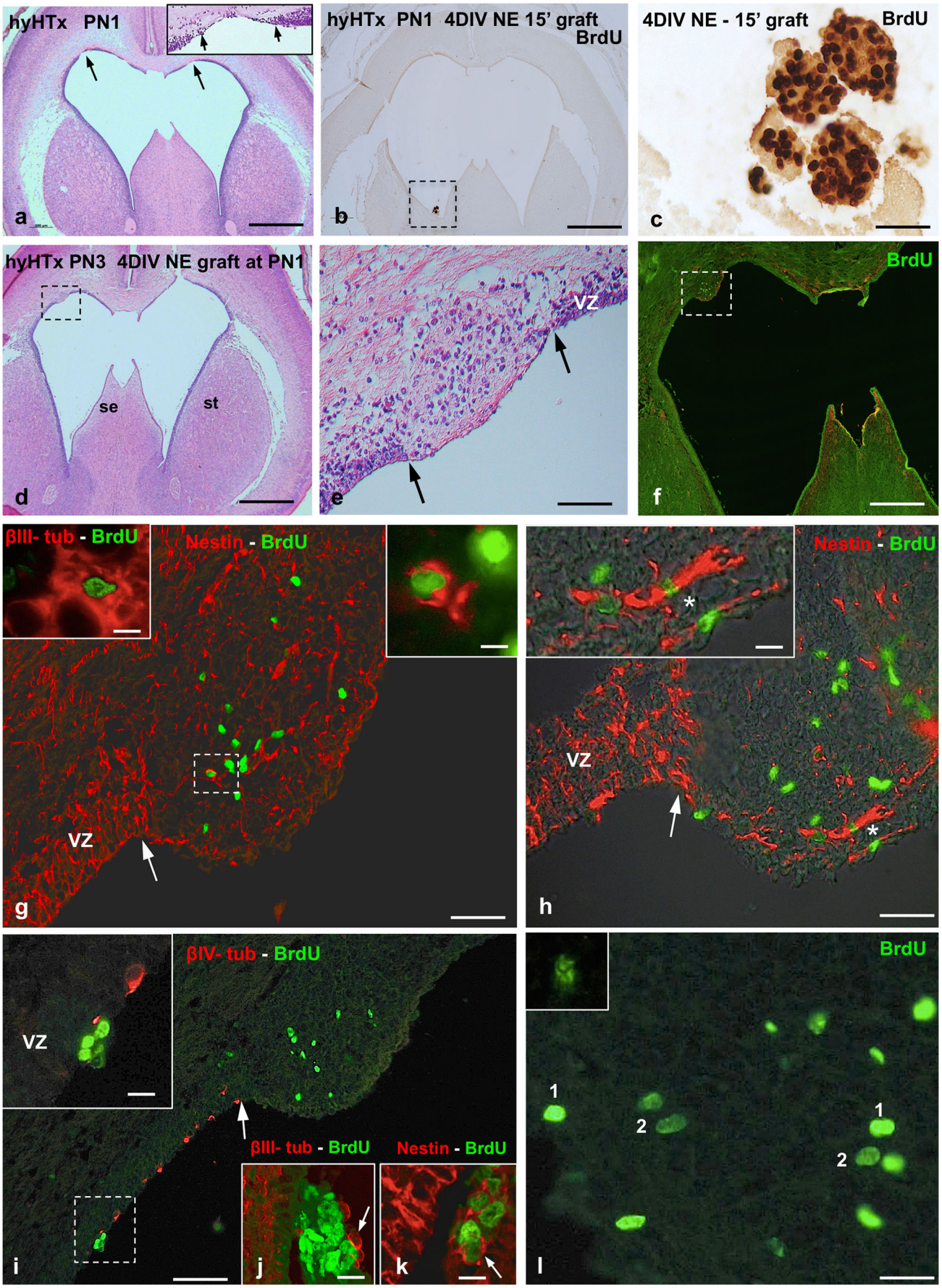
hyHTx PN1
a
hyHTx PN1 4DIV NE 15' graft
BrdU
b
4DIV NE - 15' graft
BrdU
c
hyHTx PN3 4DIV NE graft at PN1
se
st
d
VZ
e
BrdU
f
βIII- tub - BrdU
Nestin - BrdU
VZ
g
Nestin - BrdU
*
VZ
*
h
βIV- tub - BrdU
VZ
βIII- tub - BrdU
Nestin - BrdU
i
j
k
BrdU
1
2
1
2
l

Biotechnology Inc., CA, USA), dilution 1:50. Antibodies were diluted in a buffer containing 0.1 M Tris buffer, pH 7.8, 0.7% non-gelling seaweed gelatin lambda carrageenan and 0.5% Triton X-100. Corresponding secondary antibodies conjugated with Alexa Fluor 488 or 594 (1:500, Invitrogen, Carlsbad, CA) were used. In some cases, the samples were incubated with a DAPI solution (4′, 6-diamidino-2-phenylindole, dihydrochloride, Molecular ProbesTM, Thermo Fisher scientific) for 10 min. Slides were coverslipped by using a Vectashield mounting medium (Dako, Santa Clara, CA, USA) and inspected under an epifluorescence microscope to study co-localization by using the multidimensional acquisition software AxioVision Rel version 4.6 (Zeiss, Aalen, Germany) or a confocal microscope (LSM700/Axio Imager Z2m). Incubation was carried out at room temperature, 18 h. Omission of the primary antibody during incubation provided the control for the immunoreaction.

Whole mount immunofluorescence

Floating neurospheres, 6DIV and tissue blocks of the dorsal wall of the lateral ventricles of PN7 hyHTx rats were fixed in 2% paraformaldehyde in PBS, pH 7.4, for 15 min at RT and then post-fixed in 4% paraformaldehyde, in PBS pH 7.4, for 15 min and then sequentially incubated with anti-nestin (1:20 dilution)/anti-caveolin 1 (1:50 dilution) and secondary antibody conjugated with Alexa. The brains of four PN7 hyHTx rats were fixed by immersion in 4% paraformaldehyde and the roof of the lateral ventricles was processed for whole-mount immunofluorescence for βIV-tubulin.

Scanning electron microscopy

Brains from three PN5 hyHTx were fixed in 1% paraformaldehyde in 0.1 M phosphate buffer, pH 7.4, for 2 h. Tissue blocks of the dorsal roof of the dilated lateral ventricles were critical point–dried and ion-coated.

Results

Experimental design

NSCs/NPCs obtained from the VZ and SVZ of non-hydrocephalic HTx rats (nHTx) were cultured for 4 (4DIV) or 6 (6DIV) days to obtain neurospheres (Fig. 1a–e). Four and 6 DIV NEs were BrdU-labelled during the last 24 h of culture and then transplanted into a lateral ventricle of hyHTx rats, at PN1, PN2 and PN7 (Fig. 1f–i). Twenty-nine out of the 62 grafting experiments were regarded successful considering the presence of neurospheres or NSCs/NPCs in the ventricles and periventricular structures and survival of the operated rats.

The fate of the grafted NSCs/NPCs was studied by immunocytochemistry, immunofluorescence and confocal microscopy using antibodies against BrdU to trace the transplanted cells (Fig. 1i) and against cell markers: nestin (NSCs), βIII-tubulin (NPCs and neuroblasts), GFAP (astroglia), βIV-tubulin (multiciliated ependyma) and N-cadherin (adherent junctions).

The nature of the cells forming the grafted NE was investigated 15 min after grafting by immunostaining sections through the brain ventricles that contained the NE. The relative cell density of the cell types forming each NE was studied in photographs obtained at a fixed magnification (see Henzi et al. 2018). The vast majority of cells forming the grafted 4DIV and 6DIV NEs were BrdU+ (Figs. 1g, h and 2a', b' and d'–f'). A few cells located at the periphery of NE were not labelled with BrdU (Fig. 2a', a"). The grafted 4DIV NEs were formed almost exclusively by nestin+ cells. Of the total number of cells forming the grafted 6DIV NE, ~ 70% were nestin+ (NSC) (Fig. 2d, d'), ~ 12% were βIII-tubulin+ (NPC, neuron-committed cells) (Fig. 2e, e') and ~ 8% were cells with βIV-tubulin+ particles in the cytoplasm (Fig. 2f, f"); scarce GFAP+ cells (non-counted) were also present. Mitotic figures were frequent (Fig. 2b', c).

BrdU labelling of the nucleus of the grafted cell was the landmark to follow the paths and fates of the grafted NSCs/NPCs. After days/weeks of transplantation, a varying degree of BrdU labelling was evident at all target sites reached by these cells. A gradient from a strong to a fading BrdU

Fig. 4 Two days after grafting 6DIV NEs into the ventricle of PN7 hyHTx rats, the transplanted NSCs/NPCs selectively occupy the areas of VZ disruption and advance into the adjacent brain parenchyma (**g**–**I**). **a** Brain of a PN7 hyHTx fixed by vascular perfusion. A coronal section through the telencephalon shows the dilated lateral ventricles. The arrow points to the surface viewed using SEM (b) and in block immunocytochemistry (d). **b** SEM of the roof of lateral ventricles of a PN5 hyHTx rat. Asterisks indicate areas of VZ disruption. **c** Coronal paraffin section through the telencephalon of E20 hyHTx rat showing a focus of VZ disruption (df) delimited by arrows. **d** In block immunocytochemistry for βIV-tubulin of the telencephalon of a PN7 hyHTx rat. df, denudation focus; E, multiciliated ependyma. **e** Detailed magnification of a denudation focus (df) of the specimen shown in (b). **f** Paraffin section through a disruption focus (df, arrows) of a PN7 hyHTx rat showing the absence of βIV-tubulin+ ependyma. **g** PN9 hyHTx rat grafted with 6DVNEs at PN 7. Some of the grafted cells occupy the denuded area while others move into the brain cortex. 1 to 3 decreasing intensity of BrdU labelling. df, disruption front. **h** Ependymal disruption (broken arrows) selectively populated by grafted NSC/NPC (small black arrows). Some grafted cells localized in the sub-ventricular zone (SVZ, white arrow). **i** Most grafted cells located at the denuded surface express nestin. **j** The grafted cells move from the disrupted focus along the sub-ependymal region (broken arrow). df, disruption front. **k** At the disruption focus, the grafted cells move through the sub-ventricular zone (SVZ) containing βIII-tubulin+ neural progenitor cells (broken arrow). *Inset*; at the denuded surface, there are BrdU+, βIII-tubulin+-grafted NPC (full arrow) and BrdU-, βIII-tubulin+ local NPC (broken arrow). Scale bar, **b** 600 μm; **c** 120 μm

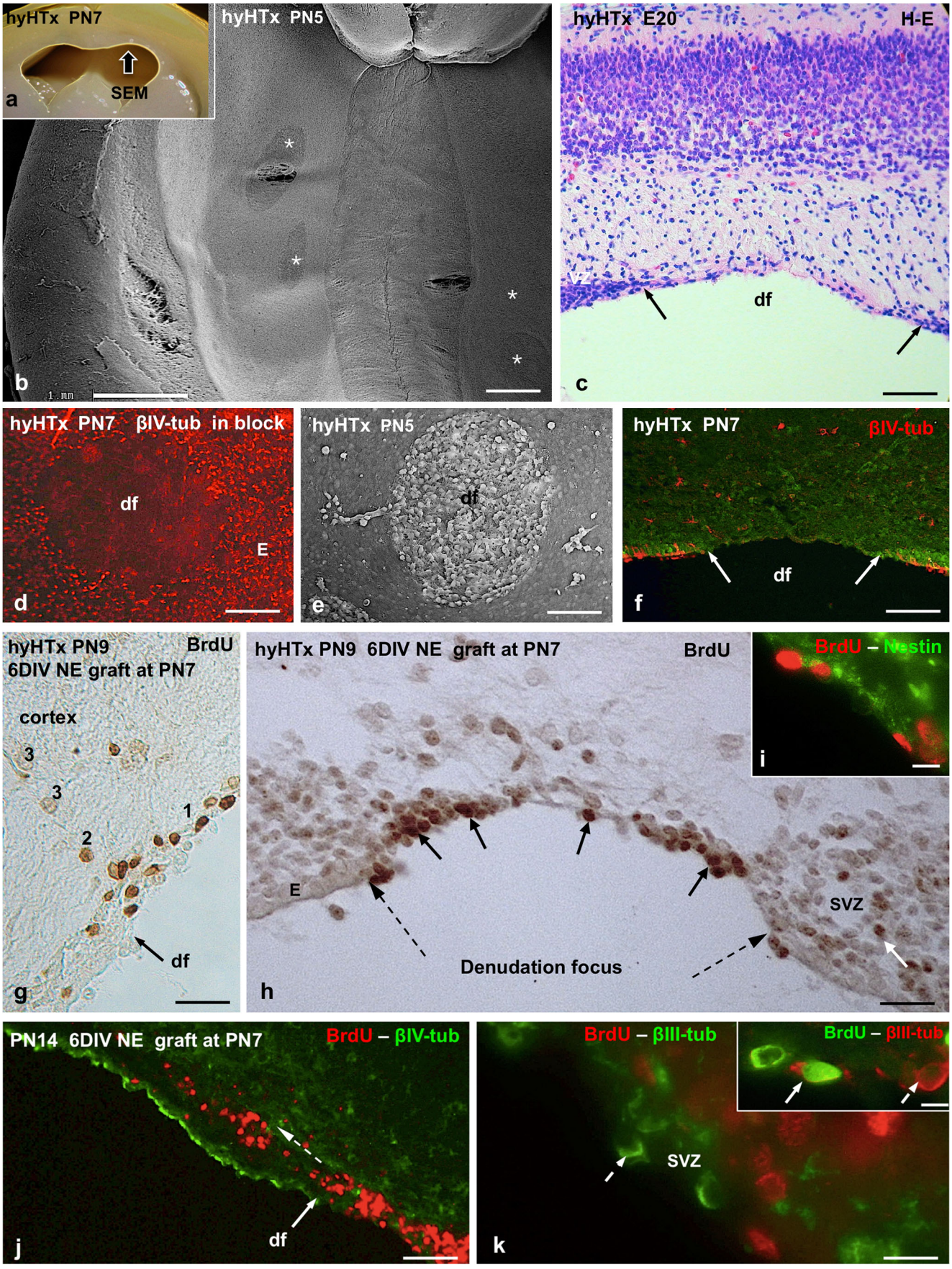
hyHTx PN7
SEM
a
hyHTx PN5
b
1 mm
hyHTx E20
H-E
VZ
df
c
hyHTx PN7 βIV-tub in block
df
E
d
hyHTx PN5
df
e
hyHTx PN7
βIV-tub
df
f
hyHTx PN9
6DIV NE graft at PN7
BrdU
cortex
3
3
1
2
df
g
hyHTx PN9 6DIV NE graft at PN7
BrdU
E
SVZ
Denudation focus
h
BrdU – Nestin
i
PN14 6DIV NE graft at PN7
BrdU – βIV-tub
df
j
BrdU – βIII-tub
SVZ
k
BrdU – βIII-tub

labelling may be regarded as a dilution of the label due to successive mitoses occurring in the NE before their disassembling and in the NE cells populating the disrupted VZ. After a few divisions, the grafted cells could no longer be traced by this strategy.

The number of NSCs/NPCs grafted to each host was relatively low, about 120,000 (6DIV NE) and 40,000 (4DIV NE). This facilitated the tracking of the transplanted cells, including their homing to the disrupted VZ.

After grafting, neurospheres remain confined to the lumen of dilated lateral ventricles

As shown by analysing serial sections through the brain, 15 min after grafting into the ventricle of PN1 and PN7 hyHTx rats, the NE remained proliferative and free inside the dilated ventricles (Figs. 2e, f and 3b, c). Although the lateral ventricles were in open communication with the third ventricle, no NEs were found in the latter at 15 min.

Two days after grafting, neurospheres disassemble and single or clustered NSTs/NPCs navigate through the CSF and home to areas of VZ disruption

Two days after grafting, 4DIV or 6DIV NEs were no longer visualized. They had disassembled into small clusters or isolated labelled cells. Clusters of BrdU+ cells were seen along the lateral wall of the lateral ventricles (Figs. 2g and 3i) and close to the areas of VZ disruption in the dorsal wall (Fig. 2h, i). In these clusters, cells expressed nestin or βIII-tubulin (Fig. 3j, k).

Graft of 4DIV neurospheres In PN1 nHTx rats, the laterodorsal wall of the ventricles displayed a distinct VZ/SVZ containing NSCs and NPCs (Fig. 1a). In PN1 hyHTx rats, VZ disruption was virtually confined to the dorsal wall of the ventricle (pallium) (Fig. 3a). Two days after surgery, NSC of 4DIV neurospheres grafted into PN1 hyHTx rats selectively populated the areas of ventricular zone disruption (Figs. 1i and 3d, g–l). At the site of VZ disruption, the grafted cells expressed nestin or βIII-tubulin (Fig. 3g, h) and their nuclei displayed different degrees of BrdU labelling (Fig. 3l).

Graft of 6DIV neurospheres Multiciliated ependymal cells formed the VZ of the lateral ventricles of PN7 hyHTx rats. Thus, in these animals, VZ disruption implies the loss of ependyma. The foci of ependyma denudation were found in the lateral and dorsal walls of the ventricles (Figs. 4a–f, 5a and 6a). Two days after grafting 6DIV NE into the ventricle of PN7 hyHTx rats, the transplanted NSCs/NPCs selectively occupied the focus of ependymal denudation occurring in the pallium (Figs. 4g, h, j and 5a, a"" and b, b'), lateral wall (Fig. 5a) and ventrally in the septum (Fig. 5c–e). Most of the grafted cells occupying the focus of ependymal denudation expressed nestin (Figs. 4i and 5a"'), while a few expressed βIII-tubulin (Fig. 4k, inset); none expressed GFAP (Fig. 5a", c').

At the denudation front, there were grafted cells with morphology similar to neighbour ciliated ependymal cells (Fig. 5c", inset) and expressing βIV-tubulin (Fig. 5e). In the ependyma close to the denudation focus, there were intermingled cells with BrdU+ nuclei (Fig. 5c"') and N-cadherin at the lateral plasma membrane domain (Fig. 5d).

In the denudation focus, a population of grafted cells penetrated the denuded SVZ (Fig. 4h, k) and progressed into the adjacent brain parenchyma (Fig. 4g, h). In the pallium, grafted cells penetrating the brain cortex showed a decreasing degree of BrdU labelling (Fig. 4g).

Seven days after transplantation, NSCs/NPCs populate the disrupted ependyma and differentiate into multiciliated ependymal cells

Graft of 4DIV neurospheres Seven days after surgery, NSCs/NPCs of 4DIV neurospheres grafted into PN1 hyHTx rats populated part of the area of ependyma denudation (Fig. 6a–c) and differentiated into single or patches of multiciliated cells some of which expressed βIV-tubulin (Fig. 6d, d").

Fig. 5 Two days after grafting 6DIV into the ventricle of PN7 hyHTx rats, BrdU+, NSC/NPC home at denuded areas of VZ. **a** Cross-section of the brain of PN9 hyHTx rats grafted with 6DIV NE at PN7. Immunoperoxidase staining for BrdU. The range framed in rectangle "a" is shown in (a', a", a"', a""); that of rectangle "b" is shown in (b, b') and that of rectangle "c" is shown in (c, c', c"). Asterisk indicates a large sub-ependymal cavity characteristic of HTx rats with severe hydrocephalus. se, septum; st, striatum. *Inset*: grafted cells located between a periventricular heterotopia (PH) and brain parenchyma. **a'** Grafted cells line the denuded surface of a large sub-ependymal cavity. **a"** Detailed magnification of (a'). Grafted cells line the denuded surface; no astrocytes (As) with a labelled nucleus were seen. E, ependyma. **a"'** Grafted cells express nestin (arrow). **a""** Section adjacent to those of previous figures immunostained for βIV-tubulin to reveal the multiciliated ependyma (E) and the denuded area. **b, b'** BrdU+, nestin+ cells populate the denuded neuropile of the brain cortex. For orientation, see rectangle "b" in (a). **c** The denuded surface of the septum is populated by the grafted NST/NPC. df, denudation front; E, ependyma. **c'** Detailed magnification of (c). Grafted cells line the denuded surface and some penetrate into the septum; no astrocytes (As) with a labelled nucleus were seen. **c", c"'** Section adjacent to that of (c). Immunoperoxidase staining for BrdU. Close to the disruption front (df, arrow), there are ependymal cells with BrdU-labelled nucleus. **c** Multiciliated ependyma. **d** Cuboidal cells with a BrdU nucleus display N-cadherin at the lateral plasma membrane domain (arrows). **e** βIV-tubulin+ cell with a BrdU+ nucleus is located at the denudation front (df). Scale bar, **a** 350 μm, inset 70 μm; **a'** 70 μm; **a"** 35 μm; **a"'** 30 μm; **a""** 35 μm; **b** 50 μm; **b'** 23 μm; **c** 45 μm; **c'** 20μm; **c"** 35 μm; inset 6 μm; **c"'** 13 μm; **d** 9 μm; **e** 12 μm, inset 120 μm; **d** 40 μm; **e** 40 μm; **f** 70 μm; **g** 30 μm; **h** 35 μm; **i** 12 μm, **j** 47 μm; **k** 12 μm

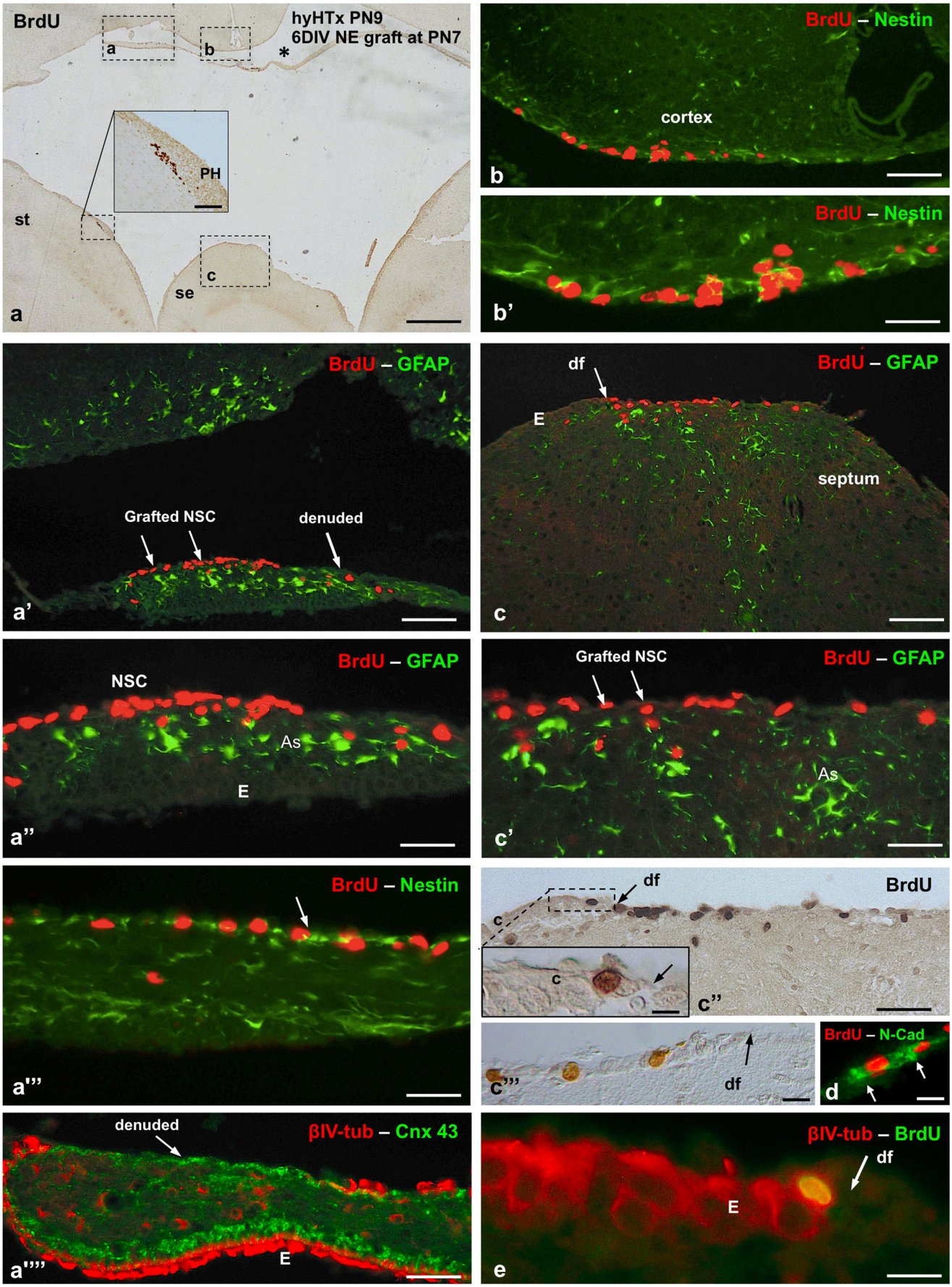
BrdU
hyHTx PN9
6DIV NE graft at PN7
a
b
*
PH
st
c
se
a
BrdU – Nestin
cortex
b
BrdU – Nestin
b'
BrdU – GFAP
Grafted NSC
denuded
a'
df
BrdU – GFAP
E
septum
c
BrdU – GFAP
NSC
As
E
a''
Grafted NSC
BrdU – GFAP
As
c'
BrdU – Nestin
a'''
df
BrdU
c
c
c''
c'''
df
BrdU – N-Cad
d
denuded
βIV-tub – Cnx 43
E
a''''
βIV-tub – BrdU
df
E
e

Figure 6(d) corresponds to a PN8 hyHTx grafted with NSCs/NPCs at PN1; an extensive area of ependymal denudation has been repopulated by βIV-tubulin+, cylindrical-multiciliated cells displaying an elongated nucleus with a decreasing gradient of BrdU labelling, suggestive of local proliferation (Fig. 6f, d, d"). The grafted cells lining denuded areas expressed N-cadherin (Fig. 6e–g).

Numerous GFAP+, BrdU astrocytes located close to the disrupted ventricular zone (Fig. 7b).

Graft of 6DIV neurospheres Seven days after grafting 6DIV NEs into the ventricle of PN7 hyHTx rats, a population of transplanted cells lined the denuded surface while another moved dorsally towards the cortex (Fig. 7a–f). The transplanted NSCs/NPCs populating the areas of ependymal denudation differentiated into ependymal cells, joined together by N-cadherin-based adherent junctions, forming a patch of new ependyma (Fig. 7e, e").

The grafted cells moving into the brain parenchyma followed the course of tissue columns weakly reactive for N-cadherin (Fig. 7e, f). Some of these grafted cells displayed a nestin+ process projecting dorsally, resembling subventricular radial glia (Fig. 7c).

Nineteen days after grafting 4DIV neurospheres into PN2 hyHTx rats only a few cells with BrdU-labelled nucleus are seen

Only two PN21 hyHTx rats grafted with 4DIV neurospheres at PN 2 were studied. The lateral ventricle showed small disruption foci "sealed" by clustered grafted cells (Fig. 7g, h). At discrete areas of the ventricular wall endowed with a continuous ependyma, cells with a varying degree of BrdU labelling of their nuclei were found intermingled with unlabelled ependymal cells, or localized in discrete sub-ependymal areas (Fig. 7i). No labelled cells were seen in other regions of the brain parenchyma.

Clusters of GFAP+, BrdU- astrocytes were seen under the ependyma displaying BrdU+ nuclei (Fig. 7i).

Discussion

For a long time, neurological impairment of patients with congenital hydrocephalus has been almost exclusively associated with damage of the brain parenchyma caused by the increased intraventricular pressure. However, derivative surgery does not resolve the neurological deficit because in these patients, the neurological impairment originates early in the embryonic life, even before hydrocephalus starts to develop (Rodríguez et al. 2012, 2019). It is necessary to distinguish between brain maldevelopment and brain damage in hydrocephalus. Brain maldevelopment is due to a primary pathology of the cells of the ventricular zone (VZ) that occurs early in development, preceding or accompanying the onset of hydrocephalus (Rodríguez et al. 2012). At variance, brain damage is a postnatal acquired defect essentially caused by ventricular hypertension, regional ischemia, disruption of white matter pathways and abnormal CSF composition that alters the microenvironment of neural cells (Del Bigio 2001, 2010). Derivative surgery, the almost exclusive treatment of hydrocephalus today, is aimed to prevent or diminish brain damage. It is clear that hydrocephalic patients improve clinically after surgery due to correction of intracranial pressure, improvement in white matter blood flow (Del Bigio 2001) and, probably, to resumption of the clearance role of CSF. However, derivative surgery does not reverse the inborn brain defects. Thirteen years ago, a study group on hydrocephalus concluded "Fifty years after the introduction of shunts for the treatment of hydrocephalus, we must acknowledge that the shunt is not a cure for hydrocephalus" (Bergsneider et al. 2006). This important reality has been underscored by three NIH-sponsored workshops on hydrocephalus (Koschnitzky et al. 2018; McAllister et al. 2015; Williams et al. 2007). Today, we can make the same statement.

Is there an alternative to derivative surgery to effectively cure foetal onset hydrocephalus? Based on the evidence that the common history of foetal onset hydrocephalus and abnormal neurogenesis are two inseparable phenomena starting early in the embryonic life with the disruption of the VZ (Domínguez-Pinos et al. 2005; Guerra et al. 2015; Jiménez et al. 2001), we explored the possibility that NSC grafting might help to diminish/repair such a disruption.

Fig. 6 Seven days after surgery, NSCs/NPCs of 4DIV neurospheres grafted into PN1, hyHTx rats home at the sites of ependyma denudation and differentiate into multiciliated cells some of which expressed βIV-tubulin. **a** PN8 hyHTx rat grafted with 4DIV NE at PN1. Haematoxylin-eosin stain. Arrows point to disrupted areas of the dorsal wall of ventricles. Areas similar to those framed in lower and upper rectangles are shown in (b) and (c), respectively. se, septum; st, striatum. **b** Grafted NSCs/NPCs accumulate at the denuded VZ delimited by arrows. **c** Transplanted cells line the area denuded of ependyma (E). 1 to 3 indicate decreasing gradient of nucleus BrdU labelling. *Inset*: labelled nuclei in ependymal cells. **d** An area of ependymal denudation (delimited by arrows) is lined by NSC/NPC grafted 7 days earlier. These cells display nuclei with a varying degree of BrdU labelling. The area framed is shown in (d'). **d'** 1 to 3 indicate decreasing gradient of BrdU labelling of the nucleus of grafted NSC/NPC forming a patch of new ependyma. **d"** A grafted cell located at the denudation front (df) has differentiated into a multiciliated βIV-tubulin+ ependymal cell. **e** Seven days after transplantation, the grafted cells homed at the denuded areas express N-cadherin, as shown in cells1 and 2. *Inset*: the same picture as in (e) but using only the channel for N-cadherin. **f** Seven days after transplantation, a grafted cell located at the denudation front (df) expresses N-cadherin. AJ, adherent junctions of ependyma. **g** Detailed magnification of a grafted cell located at the disruption front displaying N-cadherin in the cytoplasm. Scale bar, **a** 1 mm; **b** 80 μm; **c** 40 μm, inset 14 μm; **d** 46 μm; **d'** 7 μm; **d"** 9 μm; **e** 10 μm, inset 10 μm; **f** 40 μm; **g** 5 μm

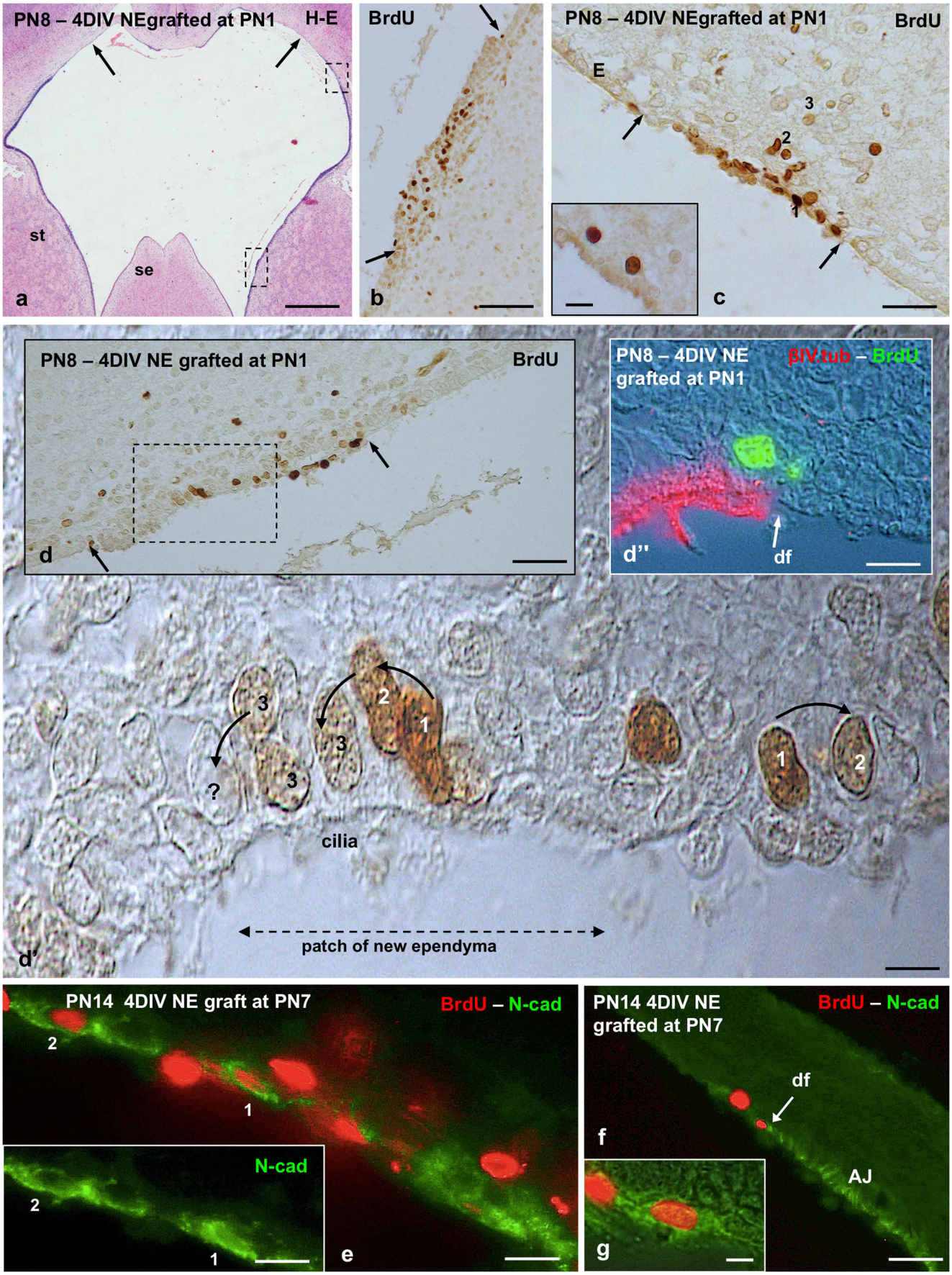
PN8 – 4DIV NEgrafted at PN1
H-E
st
se
a
BrdU
b
PN8 – 4DIV NEgrafted at PN1
BrdU
E
3
2
1
c
PN8 – 4DIV NE grafted at PN1
BrdU
d
PN8 – 4DIV NE grafted at PN1
βIV.tub – BrdU
d''
df
3
2
1
3
3
?
2
3
1
1
2
cilia
patch of new ependyma
d'
PN14 4DIV NE graft at PN7
BrdU – N-cad
2
1
N-cad
2
1
e
PN14 4DIV NE grafted at PN7
BrdU – N-cad
df
f
AJ
g

Grafting of stem cells into the cerebrospinal fluid

Although with less expectation than that of former researchers, a series of investigations continues to support the possibility that stem cell transplantation into the brain represents an opportunity for the treatment of certain neurological diseases (Armstrong and Svendsen 2000; Bjorklund and Kordower 2013; Guerra 2014; Neuhuber et al. 2008; Lindvall and Björklund 2011; Lindvall and Kokaia 2006; Politis and Lindvall 2012).

Delivery of neural stem cells/neural progenitor cells, or neurospheres, or mesenchymal stem cells (MSC) into the CSF is emerging as an alternative to grafting them in the vicinity of altered neural tissue, especially in multifocal diseases, such as multiple sclerosis. Neurospheres grafted into the ventricular CSF of mice with experimental autoimmune encephalomyelitis originate NSC/NPC that enter into demyelinating foci that differentiate into neural cells and promote multifocal re-myelination and functional recovery (Pluchino et al. 2003). In mice with induced stroke, NSCs/NPCs have been administered into the parenchyma near the infarcts and into a lateral ventricle; surprisingly, CSF administration resulted in a more efficient approach to recruit NSC/NPC to the lesion area (Kim et al. 2004). Neurospheres have been transplanted into the fourth ventricle or cisterna magna of rats with spinal cord injury. The injected cells followed the flow of subarachnoidal CSF, clustered on the pial surface of the spinal cord and a large number of them migrated into the lesion site (Bai et al. 2003; Wu et al. 2002). NSCs transplanted into the 4th ventricle of animals with injured dorsal roots reach the lesion root and become associated with axons in the same manner as Schwann cells (Ohta et al. 2004). These two experiments indicate that grafted stem cells differentiate in a site-dependent manner (Rosser et al. 2000).

A range of stem cells, such as human embryonic stem cells, human and animal neurospheres, NSC/NPC, MSC and induced pluripotent stem cells, has been used to treat Parkinson disease, stroke and other human brain disorders (Barker et al. 2016; Bjorklund and Kordower 2013; Grealish et al. 2014; Guerra 2014; Li et al. 2016; Lindvall and Björklund 2011; Lindvall and Kokaia 2006; Politis and Lindvall 2012; Satake et al. 2004; Tatarishvili et al. 2014).

Brain grafting of MSC is based on the neuroprotective and immunomodulatory properties of these cells (Fig. 8). At variance, NSC/NPC or neurospheres are grafted with the aim to replace damaged or abnormal neural cells (Fig. 8). These are two completely different strategies and aims, although complementary. In the experiments carried out by Ahn et al. (2013, 2014, 2015) on mice with induced post-haemorrhagic hydrocephalus and by Garcia-Bonilla and co-workers (2019) in *hyh* mice with spontaneous hereditary hydrocephalus, MSCs were grafted into a brain lateral ventricle (Fig. 8). Both groups reported beneficial effects on the progression of hydrocephalus triggered by anti-inflammatory and neuroprotective effects of the grafted MSC. Although in both animal models VZ disruption occurs, no reference was made to the VZ in these publications.

Presently, we used the HTx model of hereditary hydrocephalus, which expresses the mutation in about 30% of the litter (hyHTx), while the littermates develop normally (nHTx). When using the VZ/SVZ of nHTx rats as a source, neurospheres develop from neural stem cells (NSCs) and neural progenitor cells (NPCs) (Henzi et al. 2018). These two populations of NE were grafted into the CSF of hyHTx rats with the aim of achieving differentiation into neurons, glia and ependyma, as they do in vitro, diminishing/repairing the VZ disruption and its outcomes (Fig. 9).

Foetal onset hydrocephalus is triggered by a junction pathology of NSC

Mutation of several apparently non-related genes leads to a cell junction pathology of NSC and VZ disruption (Guerra et al. 2015; Rodríguez et al. 2012, 2019). All these genes impact intracellular trafficking. Their mutation causes

Fig. 7 Seven days after grafting 6DIV NEs into the ventricle of PN7 hyHTx rats, the transplanted NSCs/NPCs homed in the areas of VZ disruption differentiate into multiciliated cells some of which expressed βIV-tubulin. **a** PN14 hyHTx grafted with 6DIV neurospheres at PN7. Double immunofluorescence for BrdU (red) and GFAP (green). Grafted NSCs/NPCs populate a disruption focus of the dorsal ventricular wall. df, denudation front. **b** Adjacent section to that of (a). A population of grafted cells line the denuded surface (broken line) while another located dorsally towards the cortex (curved arrow). Numerous GFAP+, BrdU- astrocytes (As) are seen close to the disrupted ventricular zone. **c** Grafted cells display a nestin+ process projecting dorsally (solid arrow). Broken arrows point to grafted cells close to nestin+ processes. **d** In an area of ependymal denudation, some grafted cells line the exposed surface (dotted arrow) and others locate in the brain parenchyma (broken arrow). E, ependyma; df, denudation front. **e** Double immunofluorescence for BrdU (red) and N-cadherin (green). The denuded surface of a disruption focus (delimited by two arrows) is repopulated by a layer of grafted NSC/NPC expressing N-cadherin. Other grafted cells move dorsally (broken arrow). Framed area is shown in (e', e"). E, ependyma; df, disruption front. *Inset*: the same picture as (e) but using the channel for BrdU only. Arrows delimit the disruption focus. **e'** High magnification of area framed in (e). Grafted cells joined by adherent junctions (AJ) form a single layer fully occupying the denuded area. **e"** The same picture as (e') but using the channel for N-cadherin only. AJ, adherent junctions. **f** High magnification of an area of (e). Grafted cells move into the brain parenchyma following the course of tissue columns weakly reactive for N-cadherin (arrow). **g–i** PN21 hyHTx rat grafted with 4DIV neurospheres at PN2. **g**, **h** Paraffin section immunostained for BrdU and haematoxylin as background stain. The dorsal wall of a lateral ventricle shows a small disruption focus "sealed" by a cluster of grafted cells (arrow). E, ependyma. **i** In a discrete area of the ventricular wall endowed with ependyma (E), grafted cells with varying degree of BrdU labelling localize either in the ependyma proper (full and broken arrows) or in the sub-ependymal zone in close association with clusters of GFAP+, BrdU- astrocytes (As). Scale bar, **a** 47 μm; **b** 24 μm; **c** 20 μm; **d** 35 μm; **e** 40 μm; **e'**, **e"** 12 μm; **f** 20 μm; **g** 70 μm; **h** 14 μm; **i** 20 μm

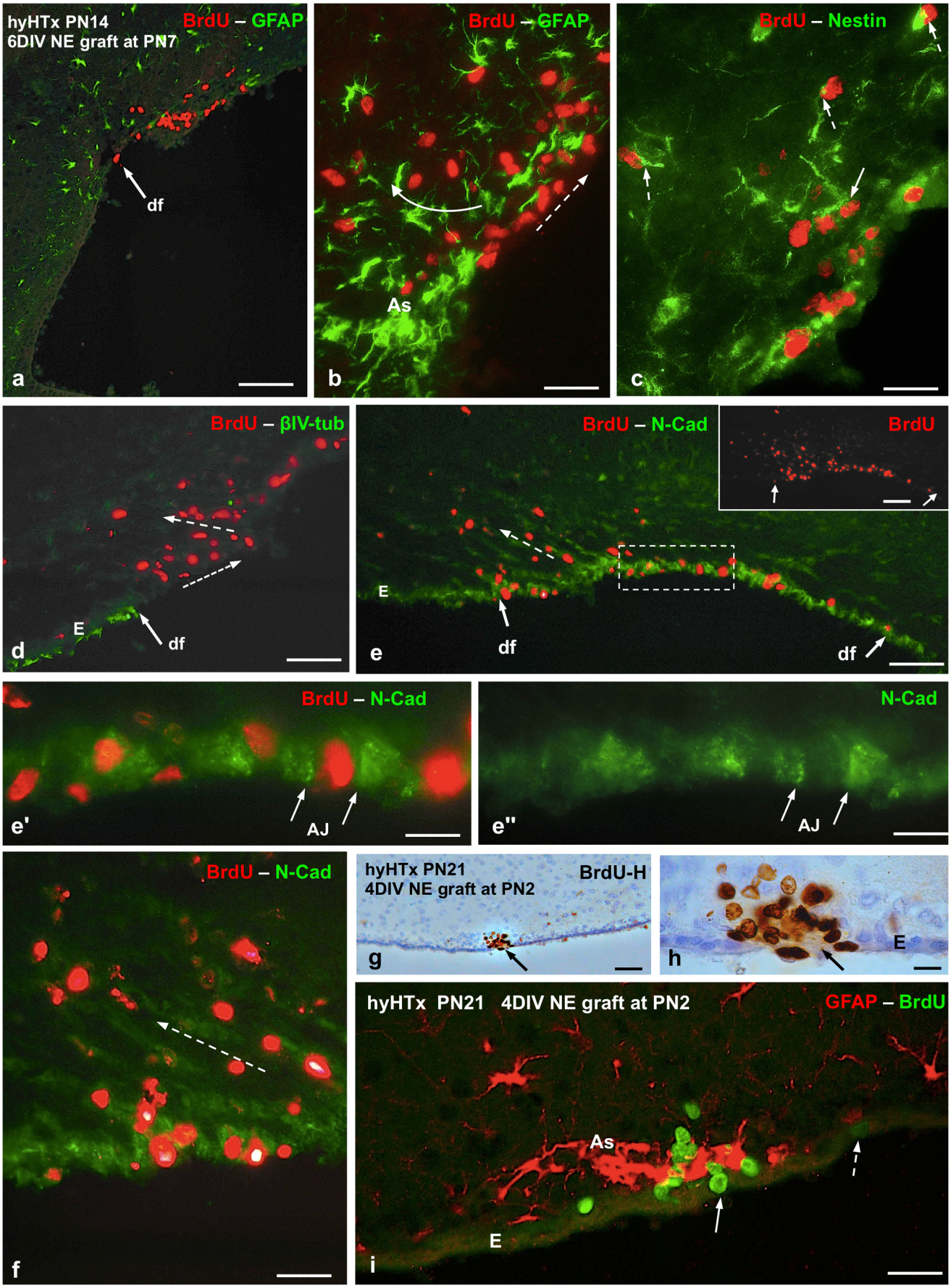
hyHTx PN14
6DIV NE graft at PN7
BrdU – GFAP
df
a
BrdU – GFAP
As
b
BrdU – Nestin
c
BrdU – βIV-tub
E
df
d
BrdU – N-Cad
BrdU
E
df
df
e
BrdU – N-Cad
e'
AJ
N-Cad
e''
AJ
BrdU – N-Cad
f
hyHTx PN21
4DIV NE graft at PN2
BrdU-H
g
E
h
hyHTx PN21 4DIV NE graft at PN2
GFAP – BrdU
As
E
i

abnormal transport of the junction proteins, N-cadherin and connexin 43, to the plasma membrane leading to disassembling of VZ, loss of NSC into CSF, abnormal migration of neuroblasts and aqueduct obliteration (Chae et al. 2004; Ferland et al. 2009; Guerra et al. 2015; Jiménez et al. 2001; Sival et al. 2011; Rodríguez et al. 2012, 2019; Wagner et al. 2003). In the telencephalon, the disrupting process results in the loss of NSC or multiciliated ependyma, abnormal neurogenesis and altered laminar CSF flow (Guerra et al. 2015; Rodríguez et al. 2019).

In hyHTx rats, NSC/NPC collected from the CSF form neurospheres that after 2 days in culture start to express a junction pathology, becoming disassembled, mirroring the pathology of the VZ in the living hyHTx (Guerra et al. 2015). This indicates that a primary genetic defect of NSC underlies the disruption phenomenon. Therefore, grafting normal NSC appears appropriate, while MSC transplantation would not solve the disruption problem.

Disruption of the VZ may also be caused by foreign signals, extrinsic to NSC. Lysophosphatidic acid, a blood-borne factor found in intraventricular haemorrhages, triggers both VZ disruption and hydrocephalus (Yung et al. 2011). Similarly, VZ disruption due to abnormal cell junctions occurs in premature neonates with intraventricular haemorrhage (McAllister et al. 2017). Finally, in vitro experiments by Castañeyra Ruiz et al. (2018) showed that immature ependymal cells exposed to blood and inhibitors of adherent junction formation exhibit impairments similar to ones demonstrated in vivo. In these cases, grafting of MSC would be expected to be beneficial, as shown by Ahn et al. (2013, 2014, 2015).

Is the hydrocephalic CSF an appropriate medium to host grafted NSC?

The foetal and adult CSF is a key component of the microenvironment of NSC during pre- and postnatal neurogenesis. Consequently, CSF would be expected to be a favourable vehicle for NSC survival. Certainly, NSC cultured in a medium containing normal foetal CSF increased survival and proliferation compared with standard culture media (Gato et al. 2005). However, the question is whether the hydrocephalic CSF, with its abnormal protein composition (Morales et al. 2015, Morales et al. 2017; Limbrick Jr et al. 2017; Ortloff et al. 2013), would be a friendly medium to host grafted NSC. Neurospheres obtained from normal HTx rats when cultured in the presence of CSF collected from normal and hydrocephalic HTx rats differentiate into neurons, astrocytes and multiciliated ependyma, indicating that the hydrocephalic CSF is a supportive medium to host NSC and that neurospheres grafted into CSF can produce neurons, glia and multiciliated ependyma (Henzi et al. 2018). Still, the definitive test to evaluate NSC/hydrocephalic CSF interaction is the grafting of NE into the CSF of living hyHTx rats.

What is actually being transplanted and when to do it?

It is required to know the essentials of the cell biology of NE as they develop in vitro in order to know what is actually being transplanted. Virtually all cells forming 4DIV NEs are proliferative, uncommitted NSC (or NPC). Under differentiation conditions, these NE generate neurons and glial cells (Henzi et al. 2018). 4DIV NEs appear suitable for grafting into the CSF since uncommitted grafted NSC/NPC would be expected to differentiate in response to clues from the host brain. At variance, in 6DIV NE, 40% of cells are committed into neuronal, glial and ependymal lineages (Henzi et al. 2018), becoming complex structures formed by cells in different phases of the cell cycle and in different states of differentiation (Bez et al. 2003; Gil-Perotín et al. 2013; Henzi et al. 2018; Marshall and Kintner 2008; Monni et al. 2011). Therefore, when grafting 6DIV NE, it should be kept in mind they are "bags" containing NSC/NPC plus cells committed into neuronal, glial and ependymal lineages.

Grafting 4DIV and 6DIV neurospheres into lateral ventricles revealed no differences in homing and differentiation into ependyma (see below). This suggests that both uncommitted and committed NSCs of the grafted 6DIV NE home similarly. Considering that 6DIV NEs have 10x more cells than 4DIV NEs and that 40% of them are already committed into neuron, glia and ependyma lineages, it may be advantageous to use them for grafting.

In the telencephalon of HTx rats, VZ disruption starts E19 as multiple foci of denudation; during 2 weeks (approximately up to PN10), these foci grow and coalesce resulting in large disrupted areas (Guerra et al. 2015; Ortloff et al. 2013). This temporal program of VZ disruption offers the possibility to perform NSC grafting postnatally, while the disruption process is still in progress. In the present investigation, NE grafting was performed at PN1 and PN2 when the disruption foci are still small and at PN7 whence the areas of VZ disruption are large. As expected, the repair efficiency of the denuded areas was higher when the animals were transplanted at younger ages.

Fate of grafted neurospheres

In hyHTx rats, the dilated lateral ventricles openly communicate with the third ventricle. However, the grafted NE remained confined to the lumen of the dilated lateral ventricles. What prevents them from moving through the interventricular foramen? Is it the disturbed CSF circulation in hydrocephalus, e.g., high pulsatility at the interventricular foramen and along the lateral walls of the lateral ventricles (Wagshul

et al. 2009; Shulyakov et al. 2012), or biochemical cues that hold them close to VZ disruption?

Between 15 min and 2 days after grafting, NEs disassemble releasing their cells into the CSF. This indicates that the CSF of hyHTx allows disassembling of NE as it does in culture (Henzi et al. 2018).

Fate of grafted NSC/NPC: navigation and homing

Sawamoto et al. (2006) showed that neuroblast migration anatomically parallels CSF flow. Ependymal cilium beating is required for normal CSF flow, concentration gradient formation of CSF guidance molecules and directional migration of neuroblasts. Ependymal cells contribute important vectorial information to guide young, migrating neurons.

NSC from NE disassembly navigate through hydrocephalus-altered CSF currents to go "back home", i.e., the ventricular zone. How do these cells orient over such a long distance? The migration, although complex, is manageable (Limbrick Jr et al. 2017; Rodríguez et al. 2019; Zappaterra et al. 2007).

Animal models such as acute and chronic spinal cord injury (SCI), traumatic brain injury (TBI) and inflammatory, genetically, or chemically induced demyelination or neurodegeneration have been used to assess the impact of NSC transplantation on lesion amelioration or tissue regeneration. CSF-injected cells confront regional fluid currents and navigate through a CSF with hundreds of signalling proteins many for signalling (Morales et al. 2012, 2015). These studies have shown a large variability in terms of migration within the host tissue. However, a common outcome is that region-specific cues dominate homing and cell fate decisions (Garzón-Muvdi and Quiñones-Hinojosa 2010; Beyer et al. 2019). Regional clues also impact the cross talk between immune cells and NSC (and their progeny) to determine efficacy of endogenous regenerative responses and the fate/functional integration of grafted NSC (Kokaia et al. 2012).The functional plasticity of the healthy CNS (including neurogenesis) depends on adaptive and innate immunity of the NSC/NPC themselves partly through expression of toll-like receptors (TLRs) (Rolls et al. 2007). Thus, the current view is that inflammation plays a key role in the homing of NSC to sites of injury or disease where certain factors such as interlukin-6, hepatic growth factor and vascular endothelial growth factor secreted by reactive astrocytes and macrophages perform a chemotactic effect (Bauer et al. 2007; Garzón-Muvdi and Quiñones-Hinojosa 2010; Takeuchi et al. 2007; Schmidt et al. 2009).

In the hydrocephalic hyh mutant mouse, myriad of macrophages were seen in areas that had undergone recent VZ disruption but they were scarce or missing from those areas that had undergone denudation early in the embryonic life. Although at lower density than that of the denuded areas, macrophages are also present in areas still endowed with VZ but that will later become denuded (Wagner et al. 2003). The

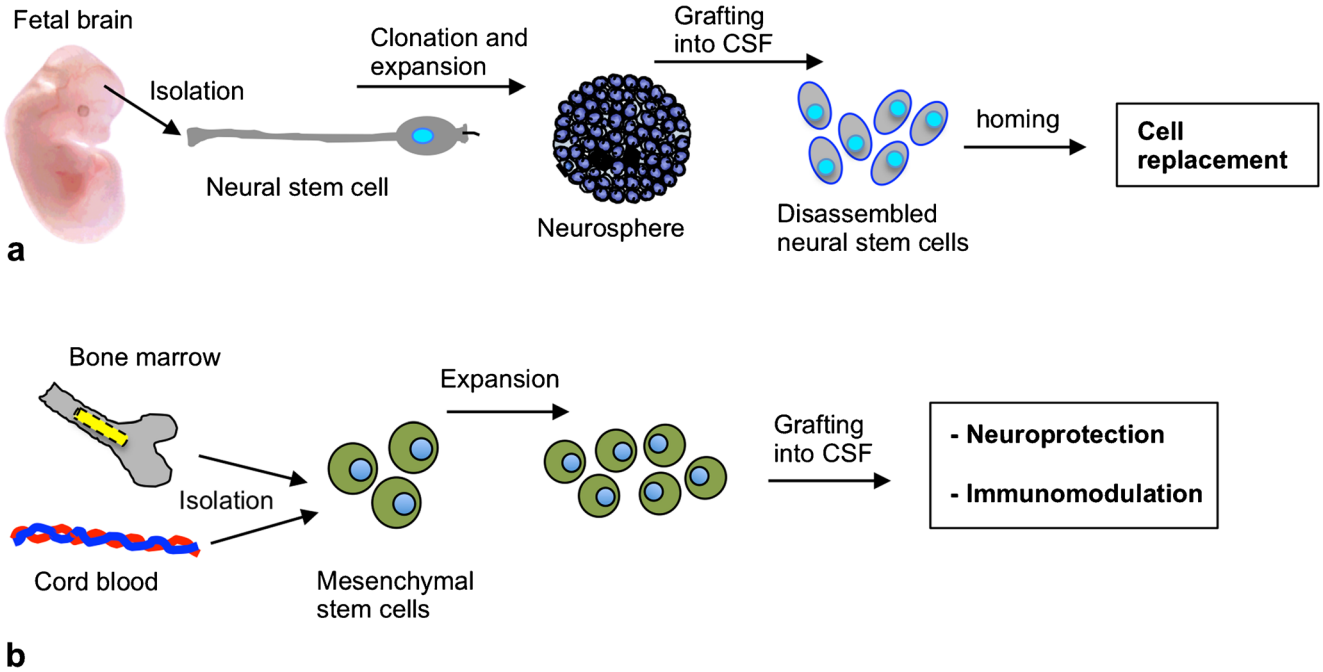

Fig. 8 Stem cells used for transplantation into the CSF of animals models of hydrocephalus. **a** NSCs/NPCs obtained from the ventricular/subventricular zones of rodent embryos or newborns are isolated and expanded to obtain neurospheres. The latter are grafted into the CSF where they disassemble releasing NSCs that home at the sites of neural disease and differentiate into neural cells. **b** Mesenchymal stem cells obtained from bone marrow or cord blood are expanded in vitro and then grafted into the CSF. They do not differentiate into neural cells but secrete factors involved in neuroprotection and immunomodulation

authors pointed to a direct relationship between onset of VZ disruption and macrophages. In the hyHTx rats, the initial steps and the progression of the VZ disruption are associated to the arrival at the areas undergoing disruption lymphocytes and macrophages and that are expressing toll-like receptors (TLR4) (Araya et al. 2013). Furthermore, interleukin-6 into the CSF is increased in hyHTx (Araya et al. 2013). It seems reasonable that cytokines released by macrophages at the VZ undergoing disruption may facilitate the homing of the grafted NSC.

In vitro and in vivo ependymogenesis

NSC and NPC of the SVZ neurogenic niche are intrinsically diverse. Human NEs display at least four different combinations of transcripts (Suslov et al. 2002) resulting in NSC and NPC with different potencies. Furthermore, the grafted 6DIV neurospheres have a heterogeneous cell population, with subpopulations committed to neural, glial and ependymal lineages (Henzi et al. 2018; present report). It is expected that the grafted NSCs homing to areas of VZ disruption do not follow a unique way of integration. Thus, while some NE cells penetrate the cortical parenchyma, others remain at the VZ and differentiate into cells most likely corresponding to multiciliated ependyma.

6DIV neurospheres derived from VZ/SVZ of PN1 nHTx (similar to those used for our grafting), further cultured in a medium without growth factors, supplemented with bovine foetal serum or hyCSF, disassemble and the free cells differentiate into neurons, astrocytes and multiciliated ependymal cells clustered by adherent junctions and displaying synchronized cilia beating (Henzi et al. 2018). A similar phenomenon seemed to occur in our in vivo experiment when NEs were grafted into hyHTx CSF, at least concerning ependymogenesis. Indeed, a population of grafted NSC homed at the disrupted VZ and differentiated into patches of ependymal cells joined by adherent junctions. Although we do not know whether their cilia (of reconstructed ependyma) actually beat, it seems likely they do considering the abovementioned in vitro results. The results obtained in

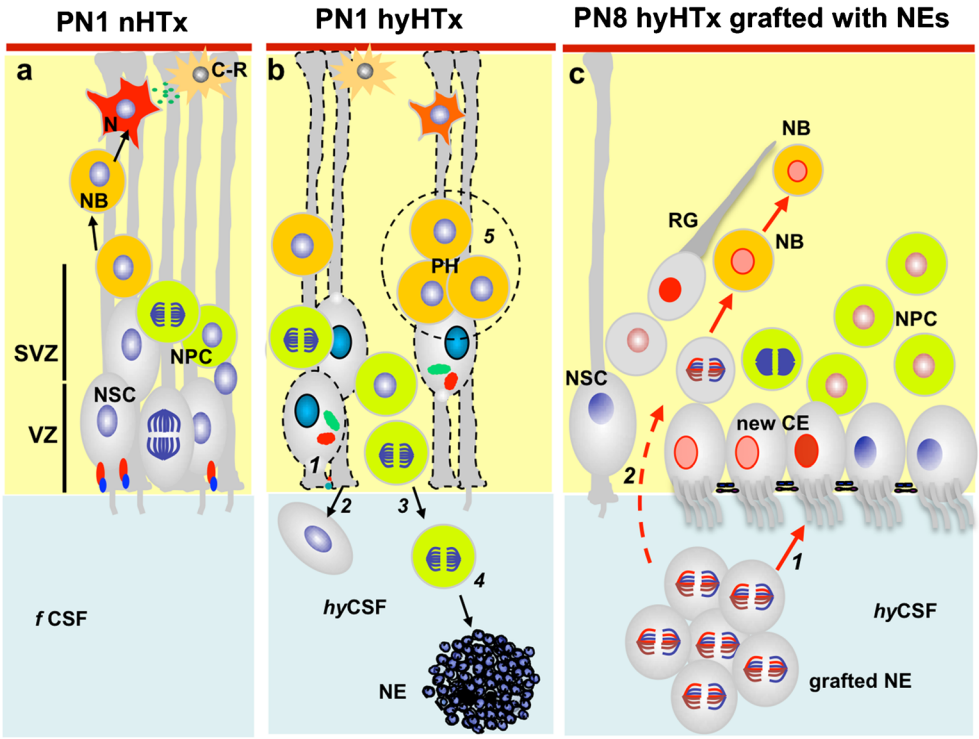

Fig. 9 Line drawing representing the cells involved in neurogenesis in the telencephalon of newborn nHTx (**a**), hyHTx (**b**) and hyHTx rats (**c**) grafted with neurospheres. **a** In nHTx rats, the ventricular zone (VZ) is formed by neural stem cells (grey, NSC), while the sub-ventricular zone (SVZ) contains proliferative neural progenitor cells (green, NPC) and neuroblasts (orange, NB). The latter migrates along radial processes of NSC and differentiates into neurons (N) that form the cerebral cortex. Cajal-Retzius cell (C-R). VZ cells are joined by adherent and gap junctions (red, blue). Specialized periventricular regions secrete signal compounds into the foetal cerebrospinal fluid (fCSF). **b** The disruption of the VZ caused by a cell junction pathology of NSC (1) results in displacement of NSC (2) and NPC (3) into the CSF (4). When collected from the CSF of hyHTx rats and cultured, these cells develop abnormal neurospheres (NEs). In the absence of the scaffold provided by NSC, neuroblasts do not migrate and form periventricular heterotopias (PH) (5). **c** After grafting neurospheres into the CSF of hyHTx rats, NSCs/NPCs (grey cells with label chromosomes) home at the disrupted VZ and, (1) differentiate into multiciliated ependyma (CE, grey cells with red nucleus), or (2) move into the parenchyma and originate neuroblasts (NB, orange cells with labelled nucleus) that associate with grafted cells with a long basal process resembling radial glia (RG). Dilution of BrdU label (nucleus in red and light red) suggests local proliferation of grafted cells

hyHTx rats grafted with NE at PN2 and studied at PN21 (the longest survival period studied) suggest that the ependyma lost in the perinatal period has been regenerated. This is further supported by ependymal presence of BrdU+ nuclei and numerous GFAP+ astrocytes; this is sort of a landmark for VZ disruption (Roales et al. 2012).

As a whole, the present findings indicate that NSC grafting into the CSF of hyHTx generate new ependyma at the sites where the ependyma is missing due to the inherited pathology (Fig. 9). The property of grafted NSC to generate ependyma should be added to the list of neuronal and glial differentiation and functional integration of transplanted NSC reported in animal models of brain diseases (Darsalia et al. 2011; Englund et al. 2002; Li et al. 2016; Pluchino et al. 2003; Tatarishvili et al. 2014; Xu et al. 2009).

A second population of grafted NSC translocated to the disrupted VZ differentiates into βIII-tubulin+ spherical cells likely corresponding to neuroblasts that "move" dorsally into the parenchyma (Fig. 9). Would they correspond to the cells that in the grafted NE are already committed to a neuronal lineage? How do they move? Do they actually migrate driven by specific clues? Do they glide along the basal process displayed by some of the partner grafted NSC? (Fig. 9). The protocol used to label the grafted cells with BrdU does not allow tracking these cells after a few mitotic divisions. Therefore, the final fate of the cells moving deep into the parenchyma and whether or not they differentiate into neurons or glia, awaits elucidation by other techniques.

Although a subpopulation of the NSC/NPC of the neurospheres used for grafting has the potency to differentiate into astrocytes (Henzi et al. 2018), in none of the transplant protocols used were GFAP+ astrocytes carrying a BrdU+ nucleus seen in the ventricular wall or brain parenchyma of hyHTx rats. Protocol limitations do not allow us to explain this phenomenon.

In conclusion, it seems possible that the new multiciliated ependyma formed after NSC/NPC grafting would help to re-establish the laminar flow of CSF and, consequently, attenuate the hydrocephalus condition. The long journey to determine that the grafted NSCs/NPCs do repair the disrupted VZ, aborting the hydrocephalic process and the abnormalities in neurogenesis, has just started.

The present study establishes an experimental paradigm of NSC/NPC therapy of foetal onset hydrocephalus, at the etiologic level, that needs to be further explored with more analytical methodologies.

Acknowledgements The authors wish to acknowledge the valuable technical support of Mr. Genaro Alvial and the Confocal and Electron Microscopy Core Facilities of Universidad Austral de Chile.

Funding information This study is supported by Fondecyt 1111018 to EMR; Hydrocephalus Association Established Investigator Award No. 51002705 to PM, EMR, CEJ and Doctoral Conicyt Fellowship (Chile) to RH.

Compliance with ethical standards

Conflict of interest The authors declare that they have no conflict of interest.

Informed consent Not applicable.

Ethical approval All procedures performed in studies involving animals were in accordance with the ethical standards of the National Research Council of Chile (Conicyt). The ethics committee of Universidad Austral de Chile approved the experimental protocol. This article does not contain any studies with human participants performed by any of the authors.

Abbreviations *AJ*, adherent junctions; *BrdU*, bromodeoxyuridine; *CE*, ciliated ependyma; *CSF*, cerebrospinal fluid; *df*, disruption front/disruption focus; *DIV*, days in vitro; E, ependyma; *GFAP*, glial fibrillary acidic protein; *GJ*, gap junctions; *hyHTx*, hydrocephalic Texas rat; *LV*, lateral ventricle; *NB*, neuroblasts; *NE*, neurospheres; *NPC*, neural progenitor cells; *NSC*, neural stem cells; *nHTx*, non-hydrocephalic Texas rat; *PH*, periventricular heterotopia; *PN*, postnatal; *se*, septum; *st*, striatum; *SVZ*, sub-ventricular zone; *VZ*, ventricular zone

References

Ahn SY, Chang YS, Sung DK, Sung SI, Yoo HS, Lee JH et al (2013) Mesenchymal stem cells prevent hydrocephalus after severe intraventricular hemorrhage. Stroke 44:497–504

Ahn SY, Chang YS, Park WS (2014) Mesenchymal stem cells transplantation for neuroprotection in preterm infants with severe intraventricular hemorrhage. Korean Journal of Pediatrics 57:251–256

Ahn SY, Chang YS, Sung DK, Sung SI, Yoo HS, Im GH, Choi SJ, Park WS (2015) Optimal route for mesenchymal stem cells transplantation after severe intraventricular hemorrhage in newborn rats. PLoS One 10(7):e0132919

Araya P, Vío K, Guerra M, Rodríguez S, Rodríguez EM (2013) An inflammatory response is associated to the progression of foetal onset hydrocephalus in the HTx rat. Procc. Int. Meeting of the Society for Research into Hydrocephalus and Spina Bifida, Cologne, Germany

Armstrong RJ, Svendsen CN (2000) Neural stem cells: from cell biology to cell replacement. Cell Transplant 9:139–152

Bai H, Suzuki Y, Noda T, Wu S, Kataoka K, Kitada K, Ohta M, Chou H, Ide C (2003) Dissemination and proliferation of neural stem cells on injection into the fourth ventricle of the rat: a trans- plantation. J Neurosci Methods 124:181–187

Baker BL (1977) Cellular composition of the human pituitary pars tuberalis as revealed by immunocytochemistry. Cell Tissue Res 182:151–163

Barker RA, Parmar M, Kirkeby A, Bjorklund A, Thompson L, Brundin P (2016) Are stem cell-based therapies for Parkinson's disease ready for the clinic in 2016? J Park Dis 6:57–63

Bauer S, Kerr BJ, Patterson PH (2007) The neuropoietic cytokine family in development, plasticity, disease and injury. Nat Rev Neurosci 8:221–232

Bergsneider M, Egnor MR, Johnston M et al (2006) What we don't (but should) know about hydrocephalus. J Neurosurg 104:157–159

Beyer F, Samper Agrelo I, Küry P (2019) Do Neural stem cells have a choice? Heterogenic outcome of cell fate acquisition in different injury models. Int J Mol Sci 20(2)

Bez A, Corsini E, Curti D, Biggiogera M, Colombo A, Nicosia RF, Pagano SF, Parati EA (2003) Neurosphere and neurosphere-forming cells: morphological and ultrastructural characterization. Brain Res 993(1–2):18–29

Bjorklund A, Kordower JH (2013) Cell therapy for Parkinson's disease: what next? Mov Disord 28:110–115

Boop FA (2004) Posthemorrhagic hydrocephalus of prematurity. In: Cinalli C, Maixner WJ, Sainte-Rose C (eds) Pediatric hydrocephalus. Springer-Verlag, Milan, Italy

Castañeyra-Ruiz L, Morales DM, McAllister JP, Brody SL, Isaacs AM, Strahle JM, Dahiya SM, Limbrick DD (2018) Blood Exposure Causes Ventricular Zone Disruption and Glial Activation In Vitro. J Neuropathol Exp Neurol 77:803–813

Chae TH, Kim S, Marz KE, Hanson PI, Walsh CA (2004) The hyh mutation uncovers roles for alpha Snap in apical protein localization and control of neural cell fate. Nat Genet 36:264–270

Darsalia V, Allison SJ, Cusulin C, Monni E, Kuzdas D, Kallur T, Lindvall O, Kokaia Z (2011) Cell number and timing of transplantation determine survival of human neural stem cell grafts in stroke-damaged rat brain. J Cereb Blood Flow Metab 31:235–242

Del Bigio MR (2001) Pathophysiologic consequences of hydrocephalus. Neurosurg Clin N Am 12:639–649

Del Bigio MR (2010) Neuropathology and structural changes in hydrocephalus. Dev Disabil Res Rev 16:16–22

Domínguez-Pinos MD, Páez P, Jiménez AJ, Weil B, Arráez MA, Pérez-Fígares JM, Rodríguez EM (2005) Ependymal denudation and alterations of the subventricular zone occur in human fetuses with a moderate communicating hydrocephalus. J Neuropathol Exp Neurol 64:595–604

Englund U, Bjorklund A, Wictorin K, Lindvall O, Kokaia M (2002) Grafted neural stem cells develop into functional pyramidal neurons and integrate into host cortical circuitry. PNAS 99:17089–17094

Ferland RJ, Bátiz LF, Neal J, Lian G, Bundock E, Lu J, Hsiao YC, Diamond R, Mei D, Banham AH, Brown PJ, Vanderburg CR, Joseph J, Hecht JL, Folkerth R, Guerrini R, Walsh CA, Rodríguez EM, Sheen VL (2009) Disruption of neural progenitors along the ventricular and subventricular zones in periventricular heterotopia. Hum Mol Genet 18:497–516

García-Bonilla M, Ojeda B, Shumilov K, Vitorica J, Guitérrez A et al (2019) Long-time effects of an experimental therapy with mesenchymal stem cells in congenital hydrocephalus. From SRHSB Abstracts, La Laguna, Tenerife, Spain

Garzón-Muvdi T, Quiñones-Hinojosa A (2010) Neural stem cell niches and homing: recruitment and integration into functional tissues. ILAR J 51:1–23

Gato A, Moro JA, Alonso MI, Bueno D, De La Mano A, Martin C (2005) Embryonic cerebrospinal fluid regulates neuroepithelial survival, proliferation, and neurogenesis in chick embryos. Anat Rec A Discov Mol Cell Evol Biol 284:475–484

Gil-Perotín S, Duran-Moreno M, Cebrián-Silla A, Ramírez M, García-Belda P, García-Verdugo JM (2013) Adult neural stem cells from the subventricular zone: a review of the neurosphere assay. Anat Rec 296:1435–1452

Grealish S, Diguet E, Kirkeby A, Mattsson B, Heuer A, Bramoulle Y, Van Camp N, Perrier AL, Hantraye P, ABjorklund A, Parmar M (2014) Human ESC-derived dopamine neurons show similar preclinical efficacy and potency to fetal neurons when grafted in a rat model of Parkinson's disease. Cell Stem Cell 15:653–665

Guerra M (2014) Neural stem cells, the hope of a better life for patients with foetal onset hydrocephalus. Fluids Barriers CNS 11:7

Guerra M, Henzi R, Ortloff A, Lichtin N, Vío K, Jimémez A, Dominguez-Pinos MD, González C, Jara MC, Hinostroza F, Rodríguez S, Jara M, Ortega E, Guerra F, Sival DA, den Dunnen WFA, Pérez-Figares JM, McAllister JP, Johanson CE, Rodríguez EM (2015) Cell junction pathology of neural stem cells is associated with ventricular zone disruption, hydrocephalus, and abnormal neurogenesis. J Neuropathol Exp Neurol 74:653–671

Henzi R, Guerra M, Vío K, González C, Herrera C, McAllister J, Johanson C, Rodriguez EM (2018) Neurospheres from neural stem/neural progenitor cells (NSPCs) of non-hydrocephalic HTx rats produce neurons, astrocytes and multiciliated ependyma. The cerebrospinal fluid of normal and hydrocephalic rats supports such a differentiation. Cell Tissue Res 373:421–438

Jellinger G (1986) Anatomopathology of non-tumoral aqueductal stenosis. J Neurosurg Sci 30:1Y16

Jiménez AJ, Tomé M, Páez P, Wagner C, Rodríguez S, Fernández-Llebrez P, Rodríguez EM, Pérez-Fígares JM (2001) A programmed ependymal denudation precedes congenital hydrocephalus in the hyh mutant mouse. J Neuropathol Exp Neurol 60:1105–1119

Johnson RT, Johnson KP, Edmonds CJ (1967) Virus-induced hydrocephalus: development of aqueductal stenosis in hamsters after mumps infection. Science 157:1066Y67

Jones HC, Klinge PM (2008) Hydrocephalus, 17-20th September, Hannover Germany: a conference report. Cerebrospinal Fluid Res 5:19

Kim DE, Schellingerhout D, Ishii K, Shah K, Weissleder R (2004) Imaging of stem cell recruitment to ischemic infarcts in a murine model. Stroke 35:952–957

Klezovitch O, Fernandez TE, Tapscott SJ, Vasioukhin V (2004) Loss of cell polarity causes severe brain dysplasia in Lgl1 knockout mice. Genes Dev 18:559–571

Kokaia Z, Martino G, Schwartz M, Lindvall O (2012) Cross-talk between neural stem cells and immune cells: the key to better brain repair? Nat Neurosci 15(8):1078–1087

Koschnitzky JE, Keep RF, Limbrick DD Jr, McAllister JP 2nd, Morris JA, Strahle J, Yung YC (2018) Opportunities in posthemorrhagic hydrocephalus research: outcomes of the Hydrocephalus Association Posthemorrhagic Hydrocephalus Workshop. Fluids Barriers CNS 15(1):11

Li W, Englund E, Widner H, Mattsson B, van Westen D, Lätt J, Rehncrona S, Brundin P, Björklund A, Lindvall O, Li J (2016) Extensive graft-derived dopaminergic innervation is maintained 24 years after transplantation in the degenerating parkinsonian brain. PNAS 113(23):6544–6549

Limbrick DD Jr, Baksh B, Morgan CD et al (2017) Cerebrospinal fluid biomarkers of infantile congenital hydrocephalus. PLoS One 12(2): e0172353

Lindvall O, Björklund A (2011) Cell therapeutics in Parkinson's disease. Neurotherapeutics 8:539–548

Lindvall O, Kokaia Z (2006) Stem cells for the treatment of neurological disorders. Nature 441:1094–1096

Lindvall O, Kokaia Z (2010) Stem cells in human neurodegenerative disorders – time for clinical translation? J Clin Invest 120:29–40

Lindvall O, Kokaia Z, Martinez-Serrano A (2004) Stem cell therapy for human neurodegenerative disorders–how to make it work. Nat Med. https://doi.org/10.1038/nm1064

Ma X, Bao J, Adelstein RS (2007) Loss of cell adhesion causes hydrocephalus in nonmuscle myosin II-B-ablated and mutated mice. Mol Biol Cell 18:2305–2312

Marshall WF, Kintner C (2008) Cilia orientation and the fluid mechanics of development. Curr Opin Cell Biol 20:48–52

McAllister JP 2nd, Williams MA, Walker ML, Kestle JR et al (2015) Hydrocephalus Symposium Expert Panel. An update on research priorities in hydrocephalus: overview of the third National Institutes of Health-sponsored symposium "Opportunities for Hydrocephalus Research: Pathways to Better Outcomes". J Neurosurg 123:1427–1438

McAllister P, Guerra M, Ruiz LC, Jimenez AJ, Dominguez-Pinos D, Sival D, den Dunnen W, Morales DM, Schmidt RE, Rodríguez

EM, Limbrick DD (2017) Ventricular zone disruption in human neonates with intraventricular hemorrhage. J Neuropathol Exp Neurol 76:358–375

Morales DM, Townsend RR, Malone JP et al (2012) Alterations in protein regulators of neurodevelopment in the cerebrospinal fluid of infants with posthemorrhagic hydrocephalus of prematurity. Molecular & Cellular proteomics 11(6):M111 011973

Morales DM, Holubkov R, Inder TE et al (2015) Cerebrospinal fluid levels of amyloid precursor protein are associated with ventricular size in post-hemorrhagic hydrocephalus of prematurity. PLoS One 10(3):e0115045

Morales DM, Silver SA, Morgan CD et al (2017) Lumbar cerebrospinal fluid biomarkers of post-hemorrhagic hydrocephalus of prematurity - amyloid precursor protein, soluble APPα, and L1 cell adhesion molecule. Neurosurgery 80(1):82–90

Neuhuber B, Barshinger AL, Paul C, Shumsky JS, Mitsui T, Fischer I (2008) Stem cell delivery by lumbar puncture as a therapeutic alternative to direct injection into injured spinal cord. J Neurosurg Spine 9:390–399

Ohta M, Suzuki Y, Noda T, Kataoka K, Chou H, Ishikawa N, Kitada M, Matsumoto N, Dezawa M, Suzuki S, Ide C (2004) Implantation of neural stem cells via cerebrospinal fluid into the injured root. Neuroreport 15:1249–1253

Ortloff A, Vío K, Guerra M, Jaramillo K, Kaehne T, Jones H, Rodríguez EM (2013) Role of the subcommissural organ in the pathogenesis of congenital hydrocephalus in the HTx rat. Cell Tissue Res 352:707–725

Pluchino S, Quattrini A, Brambilla E, Gritti A, Salani G, Dina G, Galli R, Del Carro U, Amadio S, Bergami A, Furlan R, Comi G, Vescovi AL, Martino G (2003) Injection of adult neurospheres induces recovery in a chronic model of multiple sclerosis. Nature 422:688–694

Politis M, Lindvall O (2012) Clinical application of stem cell therapy in Parkinson's disease. BMC Med 10:1

Rasin M, Gazula V, Breunig J, Kwan KY, Johnson MB, Liu-Chen S, Li HS, Jan LY, Jan YN, Rakic P, Sestan N (2007) Numb and Numbl are required for maintenance of cadherin-based adhesion and polarity of neural progenitors. Nat Neurosci 10:819–827

Roales-Buján R, Páez P, Guerra M, Rodríguez S, Vío K, Ho-Plagaro A, García-Bonilla M, Rodríguez-Pérez LM, Domínguez-Pinos MD, Rodríguez EM, Pérez-Fígares JM, Jiménez AJ (2012) Astrocytes acquire morphological and functional characteristics of ependymal cells following disruption of ependyma in hydrocephalus. Acta Neuropathol 124:531–546

Rodríguez EM, Guerra M (2017) Neural stem cells and fetal onset hydrocephalus. Pediatr Neurosurg 52:446–461

Rodríguez EM, Guerra M, Vío K, Gonzalez C, Ortloff A, Bátiz LF, Rodríguez S, Jara MC, Muñoz RI, Ortega E, Jaque J, Guerra F, Sival DA, den Dunnen WFA, Jiménez A, Domínguez-Pinos MD, Pérez-Figares JM, McAllister JP, Johanson C (2012) A cell junction pathology of neural stem cells leads to abnormal neurogenesis and hydrocephalus. Biol Res 45:231–242

Rodríguez EM, Guerra M, Ortega E (2019) Physiopathology of foetal onset hydrocephalus. In Cerebrospinal fluid disorders. lifelong implications. David Limbrick and Jeffrey Leonard (eds.). Springer International Publishing. Berna. Suiza. ISBN: 978-3-319-97928-1

Rolls A, Shechter R, London A, Ziv Y, Ronen A, Levy R, Schwartz M (2007) Toll-like receptors modulate adult hippocampal neurogenesis. Nat Cell Biol 9(9):1081–1088

Rosser AE, Tyers P, Dunnett SB (2000) The morphological development of neurons derived from EGF- and FGF-2-driven human CNS precursors depends on their site of integration in the neonatal rat brain. Eur J Neurosci 12:2405–2413

Satake K, Lou J, Lenke LG (2004) Migration of mesenchymal stem cells through cerebrospinal fluid into injured spinal cord tissue. Spine (Phila Pa 1976) 29:1971–1979

Sawamoto K, Wichterle H, Gonzalez-Perez O, Cholfin JA, Yamada M, Spassky N, Murcia NS, Garcia-Verdugo JM, Marin O, Rubenstein JL, Tessier-Lavigne M, Okano H, Alvarez-Buylla A (2006) New neurons follow the flow of cerebrospinal fluid in the adult brain. Science 311:629–632

Schmidt NO, Koeder D, Messing M, Mueller FJ, Aboody KS, Kim SU, Black PM, Carroll RS, Westphal M, Lamszus K (2009) Vascular endo- thelial growth factor-stimulated cerebral microvascular endothelial cells mediate the recruitment of neural stem cells to the neurovascular niche. Brain Res 1268:24–37

Shulyakov AV, Buist RJ, Del Bigio MR (2012) Intracranial biomechanics of acute experimental hydrocephalus in live rats. Neurosurgery 71: 1032–1040

Sival DA, Guerra M, den Dunnen WF, Bátiz LF, Alvial G, Castañeyra-Perdomo A, Rodríguez EM (2011) Neuroependymal denudation is in progress in full-term human foetal spina bifida aperta. Brain Pathol 21:163–179

Sternberger LA, Hardy PH, Cuculis JJ, Meyer HG (1970) The unlabeled antibody enzyme method of immunohistochemistry. Preparation and properties of soluble antigen-antibody complex (horseradish peroxidase-anti horseradish peroxidase) and its use in identification of spirochetes. J Histochem Cytochem 18:315–333

Suslov ON, Kukekov VG, Ignatova TN, Steindler DA (2002) Neural stem cell heterogeneity demonstrated by molecular phenotyping of clonal neurospheres. PNAS 99:14506–14511

Takeuchi H, Natsume A, Wakabayashi T, Aoshima C, Shimato S, Ito M, Ishii J, Maeda Y, Hara M, Kim SU, Yoshida J (2007) Intravenously transplanted human neural stem cells migrate to the injured spinal cord in adult mice in an SDF-1- and HGF-dependent manner. Neurosci Lett 426:69–74

Tatarishvili J, Oki K, Monni E, Koch P, Memanishvili T, Buga A, Verma V, Popa-Wagner A, Brustl O, Lindvall O, Kokaia Z (2014) Human induced pluripotent stem cells improve recovery in stroke-injured aged rats. Restor Neurol Neurosci 32:547–558

Wagner C, Batiz LF, Rodríguez S, Jiménez AJ, Páez P, Tomé M, Pérez-Fígares JM, Rodríguez EM (2003) Cellular mechanisms involved in the stenosis and obliteration of the cerebral aqueduct of hyh mutant mice developing congenital hydrocephalus. J Neuropathol Exp Neurol 62(10):1019–1040

Wagshul ME, McAllister JP, Rashid S, Li J, Egnor MR, Walker ML, Yu M, Smith SD, Zhang G, Chen JJ, Benveniste H (2009) Ventricular dilation and elevated aqueductal pulsations in a new experimental model of communicating hydrocephalus. Exp Neurol 218:33–40

Williams MA, McAllister JP, Walker ML, Kranz DA, Bergsneider M, Del Bigio MR, Fleming L, Frim DM, Gwinn K, Kestle JR, Luciano MG, Madsen JR, Oster-Granite ML, Spinella G (2007) Priorities for hydrocephalus research: report from a National Institutes of Health-sponsored workshop. J Neurosurg 107:345–357

Wu S, Suzuki Y, Noda Y, Bai H, Kitada M, Kataoka K, Nishimura Y, Ide C (2002) Immunohistochemical and electron microscopic study of invasion and differentiation in spinal cord lesion of neural stem cells grafted through cerebrospinal fluid in rat. J Neurosci Res 69:940–945

Xu L, Ryugo DK, Pongstaporn T, Johe K, Koliatsos VE (2009) Human neural stem cell grafts in the spinal cord of SOD1 transgenic rats: Differentiation and structural integration into the segmental motor circuitry. J Comp Neurol 514:297–309

Yung YC, Mutoh T, Lin ME, Noguchi K, Rivera RR, Choi JW, Kingsbury MA, Chun J (2011) Lysophosphatidic acid signaling may initiate fetal hydrocephalus. Sci Transl Med 3:99–87

Zappaterra MD, Lisgo SN, Lindsay S, Gygi SP, Walsh CA, Ballif BA (2007) A comparative proteomic analysis of human and rat embryonic cerebrospinal fluid. J Proteome Res 6:3537–3548